Structure of low-spin states in the doubly-odd ^{182}Ir nucleus

D. Hojman, J. Sauvage, B. Roussière, M.A. Cardona, G. Marguier, A. Wojtasiewicz, J. Genevey, A. Gizon, F. Ibrahim, A. Knipper, et al.

EPJ manuscript No.
(will be inserted by the editor)

Structure of low-spin states in the doubly-odd ^{182}Ir nucleus

D. Hojman[1,2,3], J. Sauvage[1], B. Roussière[1], M. A. Cardona[1,2,3,4], G. Marguier[5], A. Wojtasiewicz[6], J. Genevey[7], A. Gizon[7], F. Ibrahim[1], A. Knipper[8], F. Le Blanc[1], J. Obert[1], J. Oms[1], and the ISOLDE Collaboration

[1] Institut de Physique Nucléaire, IN2P3-CNRS/Université Paris-Sud, F-91406 Orsay cedex, France
[2] Departamento de Física, Comisión Nacional de Energía Atómica, Buenos Aires, Argentina
[3] CONICET, Buenos Aires, Argentina
[4] Escuela de Ciencia y Tecnología, Universidad de San Martín, Argentina
[5] Institut de Physique Nucléaire, Université Claude Bernard Lyon-1, F-69622 Villeurbanne cedex, France
[6] Institute of Experimental Physics, Warsaw University, Hoza 69, PL-00-681 Warsaw, Poland
[7] Laboratoire de Physique Subatomique et de Cosmologie, IN2P3-CNRS/Université Joseph Fourier, F-38026 Grenoble cedex, France
[8] Institut de Recherches Subatomiques, BP28, F-67037 Strasbourg, France

Received: date / Revised version: date

Abstract. Low-spin states of ^{182}Ir were populated through the β^+/EC decay of ^{182}Pt. Two strong $E2$ transitions were observed for the first time: a 25.7 keV transition in ^{182}Ir and a 34.0 keV transition in Re of probable mass A = 178. Spin and parity, $I^\pi = 3^+$, are firmly assigned to the ^{182}Ir ground state (g.s.). For the excited states, the parity is established and the spin determined or restricted. These assignments support most of the interpretations of the level structure previously suggested. The systematics for the known $5^+ \rightarrow 3^+$ transitions in $\pi\ h_{9/2} \otimes \nu\ 1/2^-[521]$ bands is presented. Using a semi-microscopic two-quasiparticle axial-rotor coupling model, particle configurations have been attributed or suggested for most of the coupled states lying at low energy in ^{182}Ir.

PACS. 21.10.Hw Spin, parity, and isobaric spin – 23.20.Lv γ transitions and level energies – 23.20.Nx Internal conversion and extranuclear effects – 27.70.+q $150 \leq A \leq 189$

1 Introduction

Low-spin states in ^{182}Ir have been previously investigated through the β^+/EC decay of ^{182}Pt [1]. In that work, a level scheme was established and an identification of several states was proposed based on probable multipolarities of some transitions extracted from intensity balances, theoretical arguments, and a comparison with the high-spin level scheme obtained through fusion-evaporation reactions [2]. Nevertheless, more accurate determinations of the multipolarities of the transitions are needed in order to assign spins and parities to the excited states and confirm or modify the structure assignments. In addition, in ref. [1] a special open question was the character of the 25.7 keV state. This state could have an isomeric character or correspond to the first excited state of the rotational band built on the ground state. In this context two experiments, involving measurements of internal conversion electrons, were carried out to firmly assign spin and parity values to the low-spin states in ^{182}Ir. In parallel, laser spectroscopy measurements were performed. They provided the mean square charge radius change $\delta < r^2 >$ of ^{182}Ir relatively to ^{191}Ir, which leads to a deformation parameter $< \beta^2 >^{1/2} = 0.202$ for the ^{182}Ir ground state [3]. Furthermore, the measured magnetic and spectroscopic quadrupole moments confirmed the spin value and the $\pi h_{9/2} \otimes \nu\ 1/2^-[521]$ configuration previously proposed in ref. [1] for the ^{182}Ir ground state.

In this paper, after a description of the experimental procedures in section 2, the obtained data will be given in section 3. Then, the results will be discussed and compared with microscopic theoretical predictions for a deformation close to the experimental value in order to determine the structure of the low-lying states. The structure of the states linked by the 34.0 keV E2 transition in Re will also be discussed.

2 Experimental procedures

Two decay experiments were performed to investigate the multipolarities of the transitions belonging to ^{182}Ir. In both experiments, excited levels of ^{182}Ir were populated by β^+/EC decay of ^{182}Pt nuclei ($T_{1/2}$ = 2.2 m) which, in turn, were obtained through the decay of ^{182}Hg mass separated sources. The mercury isotopes were produced by bombarding a molten lead target [4] with a 1 GeV proton beam delivered by the CERN PS Booster. The target

was connected to a plasma ion source and the 60 kV extracted ion beam was mass-separated by ISOLDE. In the first experiment, corresponding to high-resolution electron measurements, the ^{182}Hg ions were slowed down from 60 kV to 700 V using a decelerating lens before being collected on the Al deposits of the insulated tape used for the source transport. This prevents a deep implantation of the ions in the tape enabling high energy-resolution measurements for the very low-energy electrons. The radioactive ^{182}Hg sources were transported into a 180° magnetic spectrograph [5] where a preacceleration high voltage (V = -13 kV) was applied to accelerate the conversion electrons emitted by the sources. Thus the very low-energy electrons could overcome the energy cutoff due to the minimum radius of the spectrograph and reach the photographic film used as detector [6,7]. The magnetic induction applied was B = 60×10^{-4} T. The collection (t_c), waiting (t_w), and measurement (t_m) times were: t_c = 270 s, t_w = 60 s, and t_m = 330 s. More details on the experimental procedure and on the data analysis can be found in refs. [6,7]. The electron energy range was 0.6 - 106.1 keV. In the second experiment, the radioactive sources were transported to a detection station where e^--γ coincidence measurements were performed and γ and e^- singles spectra were acquired. Here, a cooled 3 mm thick Si(Li) detector and a coaxial Ge(HP) 18% efficiency detector were used for the electron and γ detection, respectively. A total of 25×10^6 coincidence events were recorded in an event-by-event mode. In this experiment we used t_c = 15 s, t_w = 115 s, and t_m = 130 s.

3 Experimental results

In fig. 1 we show a partial high-resolution electron singles spectrum obtained in the first experiment. The L and M lines for each transition are very well resolved. Among other lines, we can clearly observe the strong lines corresponding to the 25.7 keV transition, which had not been observed in the previous work [1]. Moreover, in the e^--γ experiment, the 25.7 keV M and N lines were observed in coincidence with the 81.5 keV (see fig. 2) and 45.3 keV γ-rays, confirming the existence of the proposed 25.7 keV state. The results obtained from e^--γ coincidence spectra are in agreement with those corresponding to the γ-γ coincidence experiment [1].

For different energy ranges, internal conversion coefficients (ICC) were obtained using: a) γ and spectrograph electron singles spectra, b) γ and Si(Li) electron singles spectra, and c) e^--γ and γ-γ coincidence spectra, gated on the same transitions. The normalization factors used for the evaluation of the ICC values were calculated in a self-consistent way using several stretched transitions belonging to ^{182}Ir with unambiguous multipolarities. ICC ratios were calculated using spectrograph or Si(Li) electron singles spectra or electron spectra gated on γ transitions. The experimental ICC ratios or ICC, and the theoretical values for comparison, the assigned multipolarity, the γ and total intensities, and the initial state are presented

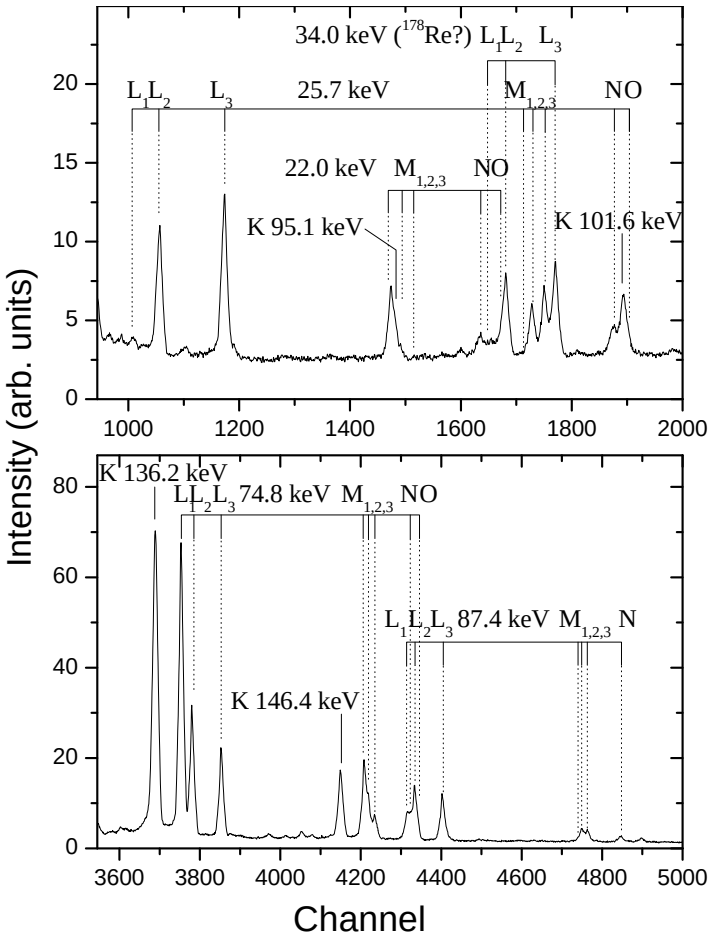

Fig. 1. Partial spectrograph electron singles spectrum.

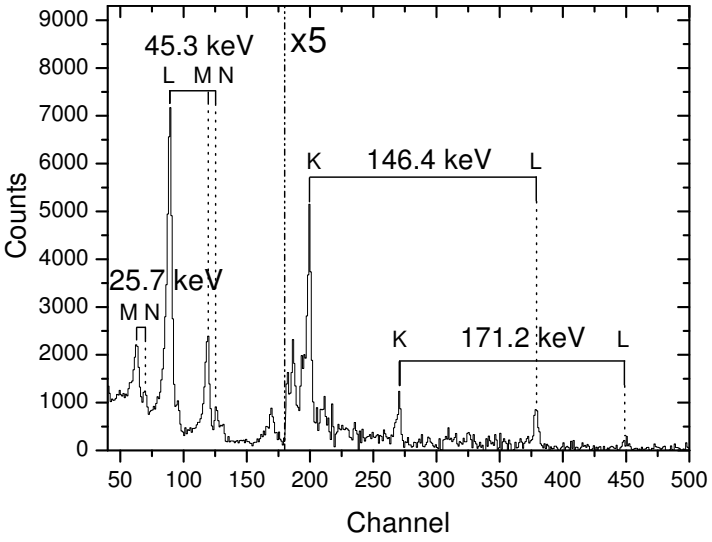

Fig. 2. e^- coincidence spectrum gated on the γ-ray corresponding to the 81.5 keV transition.

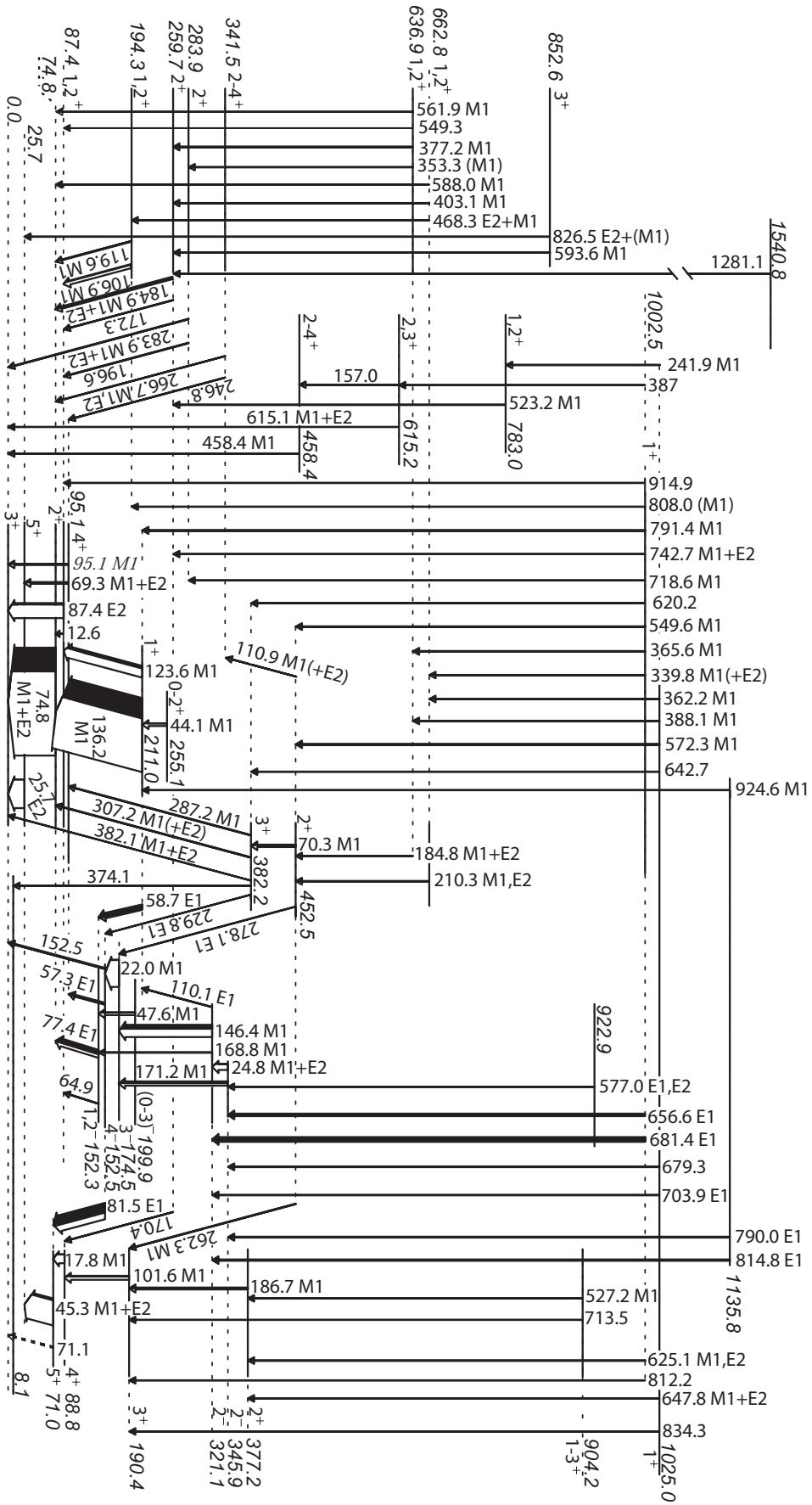

Fig. 3. Level scheme of ^{182}Ir proposed in the present work.

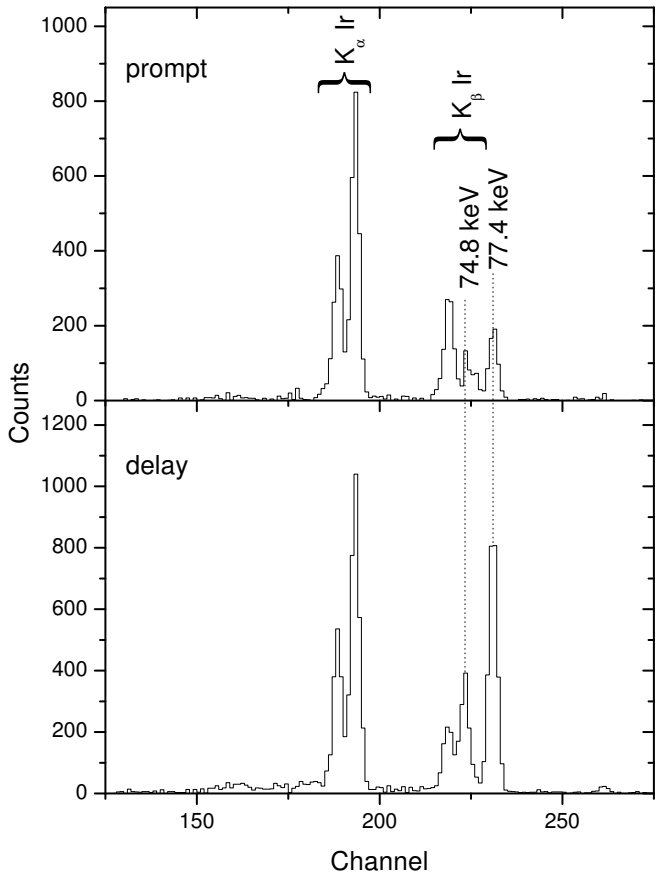

Fig. 4. Partial γ spectra in prompt and delayed coincidence with the 58.7 keV transition on the start detector.

in table 1 for transitions belonging to ^{182}Ir. The theoretical ICC values were obtained using the HSICC code from National Nuclear Data Center, Brookhaven National Laboratory, USA.

Before the present work no information about the spin and parity of the ground state of ^{182}Ir was available. In the study of the even-even nucleus ^{182}Os through the β^+/EC decay of ^{182}Ir [8], lower limits for the log f$_0$t values were obtained for the 126.9 keV ($I^\pi = 2^+$) and 400.4 keV ($I^\pi = 4^+$) states in ^{182}Os, 6.47 and 6.65 respectively. The transitions belonging to the ^{182}Os $\rightarrow$ ^{182}Ir decay and not placed in the ^{182}Ir level scheme, represent a small part of the total intensity, consequently the lower limits obtained for the log f$_0$t could be assumed as the log f$_0$t values. According to the systematics of log ft [9], the β-decays to these two levels correspond to allowed or first non-unique forbidden transitions and fix the spin of the ^{182}Ir ground state, $I_{gs} = 3$, but the parity remains uncertain. Nevertheless, the log ft value of the β-decay to the 211.0 keV state in ^{182}Ir (see table 2) corresponds to an allowed transition and, hence, unambiguously fixes the spin and parity of this state, $I^\pi = 1^+$. In addition, the $M1-E2$ character of the 136.2 and 74.8 keV transitions (the same analysis can be carried out with the other sequences linking the 211.0 keV state to the ground state) implies the same parity for the 211.0 keV and the ground states, being, finally, $I^\pi_{gs} = 3^+$. The other log ft values obtained in the present work correspond (see table 2) to the β-decays to the 1002.5 and 1025.0 keV states, indicating that these transitions are of allowed or first non-unique forbidden type, restricting the spin and parity of these states to 0^-, 1^-, or 1^+. The ICC values obtained for almost all transitions belonging to ^{182}Ir (see table 1) fix the parity of all the states, except that of the tentative level located at 8.1 keV, and fix, or restrict, their spins. As discussed in ref. [1], the 25.7 keV state could correspond to the 5^+ state of the $\pi h_{9/2} \otimes \nu\ 1/2^-[521]$ band and the 3^+ state of this configuration is expected to be located below and very close to the 5^+ state. Thus, the ground state is a good candidate for that 3^+ state. Several arguments support this assignment: a) the spin and parity of the g.s. are the correct ones, b) the 25.7 keV state depopulates to the g.s. through a strong 25.7 keV $E2$ transition in coincidence with the 45.3 keV γ line, c) laser spectroscopy measurements confirmed the spin value and configuration of the ground state, d) the population of the 2^+ and 4^+ states of ^{182}Os is in agreement with a spin value $I_{gs} = 3$. In addition, from in-beam spectroscopy [2,11] only a spin value $I = 5$ can be assigned to the 71.0 keV state. Therefore, the spin and parity values reported in the level scheme have been determined from the 3^+ ground state, 5^+ state located at 71.0 keV, 1^+ states at 211.0, 1002.5, and 1025.0 keV, and the transition multipolarities reported in table 1. Thus the spin and parity values were unambiguously determined for 20 of the 36 levels of the level scheme (fig. 3). They support most of the spin and parity assumptions as well as most of the structure assignments suggested in ref. [1]. The only changes that must be introduced are: 1) the 4^+ state of the h$_{9/2} \otimes 7/2^-[514]$ configuration changes its energy from 172.6 keV to 88.8 keV, due to the inversion of the 17.8 keV and 101.6 keV transitions in the level scheme; 2) the 152.3 keV level changes its spin from 3 to 1 or 2; 3) the 174.5 keV level has spin and parity values $I^\pi = 3^-$; and 4) the 152.5 keV level has $I^\pi = 4^-$, in agreement with the spin and parity assignments suggested in ref. [11]. In fig. 4 we show partial γ spectra in prompt and delayed coincidence with the 58.7 keV transition on the start detector. The greater intensities of the 74.8 and 77.4 keV lines in the delay spectrum compared to the prompt one clearly indicate that the 152.3 keV level corresponds to an isomeric state with a half-life shorter than that of the 152.5 keV state.

We have to note that 3 lines have been observed in the high-resolution electron singles spectrum that have the adequate energies and relative intensities to correspond to the L1, L2, and L3 internal conversion lines of a 34.0 keV $E2$ transition belonging to a Re isotope (see fig.1). Moreover, these lines are in coincidence with the Re X-rays. This 34.0 keV transition very likely belongs to ^{178}Re that is the most abundant Re isotope present in these experiments due to the counting cycle conditions and the half-lives of the ^{178,182}Os nuclei.

Table 1. γ-ray and conversion-electron data for the decay of ^{182}Pt $\rightarrow$ ^{182}Ir. The total intensities are determined using the assigned multipolarities indicated in column 6.

E_γ (keV)	ICC_{exp} or ratio	Theory $E1$	Theory $E2$	Theory $M1$	Mult.	I_γ	I_T	Initial state (keV)
12.6					$M1$,$E2$[f]			87.4
17.8	$L_1/L_2 = 15(12)$ [a]	0.65	0.024	9.9	$M1$		340(70)	88.8
22.0	$\alpha_{L_1} = 54(32)$ [b]	0.93	48	67	$M1$	11(2)	1069(176)	174.5
	$\alpha_{L_3} < 2.5$ [b]	1.6	2500	0.77				
	$\alpha_{M_1} = 15(4)$ [b]	0.22	9.6	15				
	$\alpha_{M_2} = 1.8(10)$ [b]	0.21	520	1.6				
	$\alpha_{M_3} < 0.42$ [b]	0.31	640	0.19				
24.8	$L_1/L_2 = 5.3(35)$ [a]	0.90	0.021	10	$M1 + E2$		235(60)	345.9
25.7	$L_1/L_2 \leq 0.054$ [a]	0.93	0.021	10	$E2$		1121(183)	25.7
	$L_3/L_2 = 1.3(3)$ [a]	1.4	1.2	0.11				
	$M_3/M_2 = 1.4(7)$ [a]	1.4	1.2	0.11				
44.1	$\alpha_{L_1} = 10(4)$ [b]	0.23	1.1	8.5	$M1$	8.1(20)	107(27)	255.1
	$\alpha_{L_3} < 0.50$ [b]	0.19	77	0.091				
	$\alpha_{M_1} = 2.1(10)$ [b]	0.051	0.32	1.9				
45.3	$\alpha_{L_1} = 7.0(20)$ [b]	0.21	0.97	7.8	$M1 + E2$(1%)	74(11)	1029(165)	71.0
	$\alpha_{L_2} = 1.26(40)$ [b]	0.14	63	0.77				
	$\alpha_{M_1} = 1.6(4)$ [b]	0.048	0.29	1.8				
	$\alpha_{M_2} = 0.3(1)$ [b]	0.029	16	0.19				
	$\alpha_{M_3} = 0.15(8)$ [b]	0.037	17	0.021				
	$\alpha_N = 0.6(2)$ [b]							
47.6	$\alpha_{L_1} = 7.0(36)$ [b]	0.19	0.78	6.8	$M1$	10(2)	108(32)	199.9
	$\alpha_{L_2} \leq 1.7$ [b]	0.12	50	0.67				
	$\alpha_{L_3} \leq 0.38$ [b]	0.15	53	0.073				
57.3	$\alpha_{L_1} = 0.22(18)$ [b]	0.13	0.38	3.9	$E1$	58(9)	79(12)	152.5
	$\alpha_{L_3} = 0.11(8)$ [b]	0.080	21	0.041				
	$\alpha_{M_2} < 0.038$ [b]	0.014	5.1	0.096				
	$\alpha_{M_3} \leq 0.051$ [b]	0.018	5.3	0.010				
57.7[g]	$\alpha_{L_1} \leq 0.57$ [b]	0.13	0.37	3.9	$E1$	15(2)	20(3)	
	$\alpha_{L_2} < 0.22$ [b]	0.066	20	0.38				
	$\alpha_{L_3} < 0.16$ [b]	0.078	20	0.041				
58.7	$\alpha_{L_1} = 0.10(4)$ [b]	0.12	0.35	3.7	$E1$	157(22)	210(29)	211.0
	$\alpha_{L_2} = 0.08(5)$ [b]	0.063	19	0.36				
	$\alpha_{M_1} = 0.036(24)$ [b]	0.027	0.11	0.84				
64.9	$\alpha_{L_1} < 3.1$	0.096	0.26	2.7	$E1$[f]	$\approx$7	$\approx$9	152.3
	$\alpha_{L_2} < 1.0$	0.053	11	0.27				
69.3	$L_1/L_2 = 4.1(36)$ [a]	2.2	0.026	10	$M1 + E2$($\approx$4%)	16(3)	80(16)	95.1
	$\alpha_{L_1} = 2.1(9)$ [b]	0.083	0.22	2.3				
	$\alpha_{L_2} = 0.50(32)$ [b]	0.038	8.4	0.22				
70.3	$\alpha_{L_1} = 2.1(9)$ [b]	0.080	0.21	2.2	$M1$	23(5)	95(19)	452.5
	$\alpha_L = 1.4(5)$ [e]	0.16	16	2.4				
	$\alpha_{M_1} = 0.38(23)$ [b]	0.018	0.060	0.49				
	$\alpha_{M_2} \leq 0.074$ [b]	0.0079	2.0	0.053				

Table 1. Continued.

E_γ (keV)	ICC_{exp} or ratio	Theory $E1$	Theory $E2$	Theory $M1$	Mult.	I_γ	I_T	Initial state (keV)
71.1						≈ 3	$3\leq I_T \leq 62$	71.0
74.8	$\alpha_{L_1} = 1.4(2)$ [b]	0.069	0.18	1.8	$M1+E2(8\%)$	932(230)	4243(1000)	74.8
	$\alpha_{L_2} = 0.55(14)$ [b]	0.030	5.9	0.18				
	$\alpha_{L_3} = 0.38(8)$ [b]	0.033	5.5	0.018				
	$\alpha_{M_1} = 0.34(12)$ [b]	0.015	0.051	0.41				
	$\alpha_{M_2} = 0.13(7)$ [b]	0.0066	1.5	0.044				
	$\alpha_{M_3} = 0.097(33)$ [b]	0.0077	1.4	0.0046				
77.4	$\alpha_{L_1} \approx 0.11$ [b]	0.064	0.17	1.6	$E1$	170(26)	302(45)	152.3
	$\alpha_{L_2} \approx 0.08$ [b]	0.027	5.0	0.16				
	$\alpha_{L_3} \approx 0.04$ [b]	0.030	4.7	0.017				
81.5	$\alpha_K = 0.69(45)$ [b]	0.54	0.82	9.5	$E1$	370(56)	622(93)	152.5
	$\alpha_{L_1} \leq 0.074$ [b]	0.057	0.15	1.4				
	$\alpha_{L_2} \leq 0.037$ [b]	0.023	4.0	0.14				
	$\alpha_{M_1} = 0.013(9)$ [b]	0.012	0.041	0.32				
	$\alpha_{M_2} = 0.011(7)$ [b]	0.0051	0.99	0.034				
	$\alpha_{M_3} = 0.009(6)$ [b]	0.0058	0.93	0.0036				
87.4	$\alpha_K = 1.1(8)$ [b]	0.46	0.85	7.7	$E2$	64(10)	591(89)	87.4
	$\alpha_{L_{1-2}} = 3.3(16)$ [b]	0.064	3.0	1.3				
	$\alpha_{L_3} = 3.0(12)$ [b]	0.020	2.6	0.012				
	$\alpha_{M_1} \leq 0.093$ [b]	0.011	0.034	0.26				
	$\alpha_{M_2} = 0.96(48)$ [b]	0.0041	0.71	0.028				
	$\alpha_{M_3} = 0.83(41)$ [b]	0.0047	0.66	0.0029				
95.1	$\alpha_K = 5.8(27)$ [b]	0.37	0.81	6.0	$M1$	5.8(10)	48(10)	95.1
	$\alpha_{L_1} = 1.1(7)$ [b]	0.039	0.11	0.90				
96.9[g]	$\alpha_K \approx 5$ [b]	0.35	0.79	5.7	$(M1)$	3.2(15)	26(18)	
101.6	$\alpha_K = 6.6(20)$ [b]	0.31	0.75	5.0	$M1$	22(3)	156(31)	190.4
	$\alpha_{L_1} = 1.0(4)$ [b]	0.034	0.096	0.74				
	$\alpha_{M_1} = 0.32(20)$ [b]	0.0074	0.024	0.17				
106.9	$\alpha_K = 5.0(15)$ [b]	0.28	0.70	4.3	$M1$	25(4)	156(31)	194.3
	$\alpha_K = 3.2(7)$ [e]							
	$\alpha_{L_1} = 0.81(48)$ [b]	0.030	0.086	0.64				
	$\alpha_L = 0.77(20)$ [e]	0.050	2.2	0.71				
110.1	$\alpha_K < 1$ [b]	0.26	0.67	4.0	$E1$	8.1(12)	11(2)	321.1
	$\alpha_L \leq 0.18$ [e]	0.046	1.9	0.65				
110.9	$\alpha_K \approx 4(2)$ [b]	0.25	0.65	3.8	$M1(+E2)$	2.5(4)	$3\leq I_T \leq 14$	452.5
119.6	$\alpha_K = 3.9(33)$ [b]	0.21	0.57	3.1	$M1$	6.3(10)	30(9)	194.3
123.6	$\alpha_K = 3.1(5)$ [b]	0.19	0.54	2.8	$M1$	100(10)	446(67)	211.0
	$\alpha_K = 2.5(5)$ [e]							
	$\alpha_L = 0.47(13)$ [e]	0.034	1.1	0.47				
	$\alpha_M = 0.21(6)$ [e]	0.0077	0.28	0.11				
136.2	$\alpha_K = 2.1(3)$ [b]	0.15	0.44	2.2	$M1$	777(93)	2810(562)	211.0
146.4	$\alpha_K = 2.0(3)$ [b]	0.12	0.37	1.8	$M1$	154(23)	481(72)	321.1

Table 1. Continued.

E_γ (keV)	ICC_{exp} or ratio	Theory $E1$	Theory $E2$	Theory $M1$	Mult.	I_γ	I_T	Initial state (keV)
152.5	$\alpha_K < 0.56$ [b]	0.11	0.34	1.6	$E1$ [f]	38(6)	43(6)	152.5
157.0						2.2(3)	$2\leq I_T \leq 6$	615.2
168.8	$\alpha_K = 1.2(8)$ [b] $\alpha_K = 1.0(5)$ [e]	0.087	0.26	1.2	$M1$	6.5(10)	16(4)	321.1
170.4[g]						5.2(8)	$6\leq I_T \leq 12$	
171.2	$\alpha_K = 1.4(7)$ [b] $\alpha_K = 1.0(1)$ [e] $\alpha_L = 0.18(4)$ [e]	0.083 0.014	0.25 0.26	1.1 0.18	$M1$	71(11)	168(25)	345.9
172.3					$M1, E2$ [f]	6.8(10)	$7\leq I_T \leq 16$	259.7
184.8	K/L = 7.0(47) [d] $\alpha_K = 0.77(29)$ [e] $\alpha_L = 0.11(6)$ [e]	6.0 0.070 0.012	1.1 0.21 0.19	6.2 0.93 0.15	$M1 + E2$	6.5(10)	12(4)	636.9
184.9	K/L = 4.2(19) [d] $\alpha_K = 0.77(32)$ [e] $\alpha_L = 0.18(8)$ [e]	6.0 0.070 0.012	1.1 0.21 0.19	6.2 0.93 0.15	$M1 + E2$	49(7)	94(23)	259.7
186.7	K/L = 6.2(21) [d] $\alpha_K = 0.94(40)$ [c] $\alpha_K = 0.90(37)$ [e] $\alpha_L = 0.14(7)$[e]	6.0 0.067 0.011	1.1 0.20 0.18	6.2 0.89 0.14	$M1$	36(5)	75(15)	377.2
196.6						13.5(20)	$12\leq I_T \leq 30$	283.9
210.3	$0.10 \leq \alpha_K \leq 1.2$ [e]	0.050	0.15	0.63	$M1, E2$	14(2)	20(6)	662.8
229.8	$\alpha_K \approx 0.06$ [e]	0.040	0.12	0.50	$E1$	4.6(14)	5(2)	382.2
241.9	$\alpha_K = 0.48(13)$ [c]	0.035	0.11	0.43	$M1$	5.3(8)	8(2)	1025.0
246.8						6.6(10)	9(3)	341.5
262.3	K/L = 4.7(42) [d] $\alpha_K = 0.32(17)$ [e] $\alpha_L = 0.068(54)$ [e]	6.2 0.029 0.0047	1.9 0.085 0.045	6.2 0.35 0.056	$M1$	15(2)	21(5)	452.5
266.7	$\alpha_K = 0.2(1)$ [c]	0.028	0.082	0.33	$M1, E2$	8(1)	10(2)	341.5
278.1	$\alpha_K < 0.06$ [e]	0.025	0.073	0.29	$E1$	12(2)	12(2)	452.5
283.9	$\alpha_K = 0.25(5)$ [c]	0.024	0.070	0.28	$M1 + E2$	18(3)	23(6)	283.9
287.2	$\alpha_K = 0.26(5)$ [c] $\alpha_K = 0.40(19)$ [e]	0.023	0.068	0.27	$M1$	16(2)	21(5)	382.2
304.5[g]	$\alpha_K \approx 0.17$ [c]	0.020	0.058	0.23	$(M1 + E2)$	3.6(8)	4.2(12)	
307.2	K/L = 3.0(25) [d] $\alpha_K = 0.23(6)$ [e] $\alpha_L = 0.067(60)$ [e]	6.3 0.020 0.0031	2.3 0.057 0.024	6.2 0.22 0.036	$M1(+E2)$	17(3)	22(5)	382.2

Table 1. Continued.

E_γ (keV)	ICC_{exp} or ratio	Theory $E1$	Theory $E2$	Theory $M1$	Mult.	I_γ	I_T	Initial state (keV)
339.8	$\alpha_K = 0.16(8)$ [e]	0.016	0.044	0.17	$M1(+E2)$	7.6(11)	9(2)	1002.5
348.5[g]						4.7(11)	5(2)	
353.3	$\alpha_K \approx 0.2$	0.014	0.040	0.15	$(M1)$	4(1)	5(1)	636.9
362.2	$\alpha_K = 0.12(3)$ [c] $\alpha_K = 0.16(6)$ [e]	0.014	0.038	0.14	$M1$	15(2)	18(4)	1025.0
365.6	$\alpha_K = 0.14(3)$ [c] $\alpha_K = 0.15(4)$ [e]	0.013	0.037	0.14	$M1$	21(3)	25(5)	1002.5
374.1	$\alpha_K \leq 0.14$ [c]	0.013	0.035	0.13		6.1(9)	7(2)	382.2
377.2	$\alpha_K = 0.13(3)$ [c] $\alpha_K = 0.20(9)$ [e] $\alpha_{L_1+L_2} = 0.020(5)$ [c]	0.012 0.0018	0.034 0.0094	0.13 0.021	$M1$	27(4)	31(6)	636.9
382.1	$\alpha_K = 0.063(20)$ [c]	0.012	0.033	0.13	$M1 + E2$	3(1)	3(1)	382.2
386.5[g]	$\alpha_K = 0.064(20)$ [c]	0.012	0.032	0.12	$M1 + E2$	3(1)	3(1)	
387						7(1)	7(1)	1002.5
388.1	$\alpha_K = 0.14(6)$ [e]	0.012	0.032	0.12	$M1$	10(2)	11(2)	1025.0
391.3[g]	$\alpha_K \leq 0.017$	0.011	0.031	0.12	$E1$	6.7(10)	7(1)	
403.1	$\alpha_K = 0.13(5)$ [e]	0.011	0.029	0.11	$M1$	10(2)	11(2)	662.8
413.2[g]	$\alpha_K = 0.085(20)$ [c]	0.010	0.028	0.10	$(M1 + E2)$	5.8(11)	6.2(14)	
417.5[g]	$\alpha_K \approx 0.13$ [e]	0.0098	0.027	0.099	$M1$	4.5(9)	4.9(10)	
423.8[g]	$\alpha_K = 0.17(8)$ [c]	0.0095	0.026	0.095	$M1$	2.7(10)	3.0(11)	
425.9[g]	$\alpha_K = 0.052(36)$ [c]	0.0094	0.026	0.094	$M1 + E2$	5.8(9)	6(1)	
450.8[g]						2.6(10)		
452.2[g]						4.4(9)		
458.4	$\alpha_K = 0.089(28)$ [c]	0.0080	0.022	0.077	$M1$	10(2)	11(2)	458.4
468.3	$\alpha_K = 0.033(11)$ [c]	0.0077	0.021	0.073	$E2 + M1$	6.5(12)	6.8(15)	662.8
472.4[g]	$\alpha_K = 0.077(20)$ [c]	0.0075	0.020	0.073	$M1$	17(3)	18(3)	
473.7[g]	$\alpha_K = 0.081(20)$	0.0075	0.020	0.071	$M1$	12(2)	13(2)	
520.2[g]	$\alpha_K = 0.053(19)$ [c]	0.0061	0.016	0.055	$M1 + E2$	8.5(13)	9(2)	
523.2	$\alpha_K = 0.071(21)$ [c]	0.0061	0.016	0.055	$M1$	9.2(14)	10(2)	783.0
527.2	$\alpha_K = 0.074(21)$ [c]	0.0060	0.016	0.054	$M1$	7.6(11)	8(2)	904.2
549.3					$M1$,E2[f]	5(1)	5(1)	636.9

Table 1. Continued.

E_γ (keV)	ICC_{exp} or ratio	Theory $E1$	$E2$	$M1$	Mult.	I_γ	I_T	Initial state (keV)
549.6	$\alpha_K = 0.060(14)$	0.0055	0.014	0.048	$M1$	17(3)	18(4)	1002.5
561.9	$\alpha_K = 0.047(14)$ [c]	0.0052	0.014	0.045	$M1$	32(4)	34(6)	636.9
572.3	$\alpha_K = 0.049(12)$ [c]	0.0050	0.013	0.043	$M1$	37(4)	39(5)	1025.0
575.0[g]						7(2)		
577.0	$\alpha_K < 0.01$ [c]	0.0049	0.013	0.042	$E1, E2$	8.9(13)	9(2)	922.9
583.7[g]	$\alpha_K \approx 0.034$ [c]	0.0048	0.013	0.041	$M1+E2$	6(2)	6(2)	
588.0	$\alpha_K \approx 0.054$ [c]	0.0048	0.012	0.040	$M1$	≈7(1)	≈7(1)	662.8
593.6	$\alpha_K = 0.047(12)$ [c]	0.0047	0.012	0.040	$M1$	9.5(14)	10(2)	852.6
615.1	$\alpha_K \approx 0.026$ [c]	0.0043	0.011	0.036	$M1+E2$	5.1(8)	5(1)	615.2
620.2	$\alpha_K \leq 0.027$ [c]	0.0043	0.011	0.035	$M1, E2$[f]	7.8(12)	8(1)	1002.5
625.1	$\alpha_K = 0.052(35)$ [c]	0.0042	0.011	0.035	$M1, E2$	15(2)	15(2)	1002.5
642.7					M1,E2[f]	8.3(12)	9(2)	1025.0
647.8	$\alpha_K = 0.028(7)$ [c]	0.0039	0.010	0.032	$M1+E2$	13(2)	13(2)	1025.0
656.6	$\alpha_K = 0.0040(10)$ [c]	0.0038	0.0098	0.030	$E1$	99(10)	99(10)	1002.5
679.3	$\alpha_K \leq 0.01$ [c]	0.0036	0.0092	0.028	$E1$[f]	23(3)	23(3)	1025.0
681.4	$\alpha_K = 0.0040(7)$ [c]	0.0035	0.0091	0.028	$E1$	180(18)	181(18)	1002.5
684.2[g]						≤6(1)	≤6(1)	
703.9	$\alpha_K < 0.007$ [c]	0.0033	0.0085	0.025	$E1$	23(3)	23(3)	1025.0
713.5	$\alpha_K < 0.05$ [c]	0.0032	0.0083	0.025	$M1, E2$[f]	3.8(6)	4(1)	904.2
718.6	$\alpha_K = 0.030(11)$ [c]	0.0032	0.0082	0.024	$M1$	6.7(10)	7(1)	1002.5
742.7	$\alpha_K = 0.020(10)$ [c]	0.0030	0.0076	0.022	$M1+E2$	4.4(7)	5(1)	1002.5
790.0	$\alpha_K = 0.0032(15)$ [c]	0.0027	0.0068	0.019	$E1$	≈34(4)	≈34(4)	1135.8
791.4	$\alpha_K = 0.031(7)$ [c]	0.0026	0.0067	0.019	$M1$	31(4)	31(4)	1002.5
808.0	$\alpha_K \approx 0.023$ [c]	0.0025	0.0065	0.018	$(M1)$	4.6(7)	5(1)	1002.5
812.2					$M1, E2$[f]	6.7(10)	7(1)	1002.5
814.8	$\alpha_K = 0.0044(15)$ [c]	0.0025	0.0064	0.018	$E1$	51(6)	51(6)	1135.8
826.5	$\alpha_K \approx 0.008$ [c]	0.0024	0.0062	0.017	$E2(+M1)$	12(2)	12(2)	852.6
834.3					$E2$[f]	7.8(12)	8(1)	1025.0

Table 1. Continued.

E_γ (keV)	ICC_{exp} or ratio	Theory $E1$	Theory $E2$	Theory $M1$	Mult.	I_γ	I_T	Initial state (keV)
914.9						11(2)	11(2)	1002.5
924.6	$\alpha_K = 0.017(7)$ [c]	0.0020	0.0050	0.013	$M1$	6.6(10)	7(1)	1135.8
1281.1						6(1)	6(1)	1540.8

[a] From spectrograph electron singles spectra.
[b] From γ and spectrograph electron singles spectra.
[c] From γ and Si(Li) electron singles spectra.
[d] From e^--γ coincidence spectra.
[e] From e^--γ and γ-γ coincidence spectra.
[f] Multipolarity deduced from the level scheme.
[g] Transition not placed in the level scheme.

Table 2. $(EC + \beta^+)$ feedings, log ft values and spin assignments in the ^{182}Pt $\rightarrow$ ^{182}Ir decay. Q = 2883(37) keV and $T_{1/2}$ = 2.2(1) m [10].

Level energy (keV)	$I(EC + \beta^+)$%	log f_0t	log f_1t
211.0	54(22)	4.6(2)	6.0(2)
1002.5	6.9(22)	5.2(1)	6.3(1)
1025.0	2.4(8)	5.6(1)	6.7(2)

4 Discussion

The structure of the levels established in ^{182}Ir has already been discussed extensively in ref. [1] but, as I^π values have been determined for most of the ^{182}Ir levels in the present work, it is interesting to compare again the experimental results with theoretical calculations performed taking into account new results obtained in this mass region since 1995. The nuclear moments and mean square charge radius changes, $\delta <r_c^2>$ of isomeric and ground states of several Pt and Ir nuclei have been extracted from laser spectroscopy measurements [3,12]. They have shown that the odd and doubly-odd nuclei located around the ^{182}Ir nucleus have a prolate shape with the following β deformation parameters: $\beta = 0.227$ for the $1/2^-[521]$ ground state of ^{183}Pt, $\beta = 0.246$ for the $7/2^-[514]$ isomeric state of ^{183}Pt, $\beta = 0.225$ for the ^{182}Pt ground state, $\beta = 0.216$ for the ^{184}Pt ground state, $\beta = 0.202$ for the ^{182,184,185,186}Ir ground states, $\beta = 0.167$ for the ^{186}Ir isomeric state, and $\beta = 0.207$ for the ^{183}Ir ground state. The deformation parameters for the ^{180,182}Os nuclei deduced from the B(E2) values of the $2_1^+ \rightarrow 0_1^+$ transition given in ref. [13] are: $\beta = 0.228$ and $\beta = 0.234$, respectively. Thus, the Ir isotopes in their ground state have very similar β values but they have weaker deformation than the Pt and Os nuclei. That means that the proton states observed in the neighboring odd-A Ir will also be present in the doubly-odd ^{182}Ir nucleus. On the other hand, for the neutron, the state order could be slightly modified by the deformation change between ^{182}Ir and ^{183}Pt and ^{181}Os nuclei. In table 3 we list the zero-order configurations deduced from the single-particle proton and neutron states observed at low energy in the neighboring odd-A nuclei and which are expected to be present in ^{182}Ir up to about 1 MeV (more details can be found in ref. [1]). In the second column of the table we report the K values obtained from the proton-neutron coupling with parallel and anti-parallel spins corresponding to energy-favored and energy-unfavored states, respectively, according to the Gallagher and Moskowski rule [14].

4.1 Brief description of theoretical calculations.

The theoretical calculations were performed using the two-quasiparticle axial-rotor semi-microscopic coupling model developed by Bennour *et al.*. [15]. In this approach the particle number is not conserved, which means that the energy location of the ^{182}Ir states can be determined from anyone of the four neighboring ^{180,182}Os or ^{182,184}Pt cores but, obviously, in all cases the Fermi level of the ^{182}Ir nucleus cannot be exactly reproduced. The variable moments of inertia used in the calculations have been deduced from the experimental energy sequences observed in the cores. To calculate the coupled states, we need the quasiparticle wave functions and the corresponding occupation probabilities, v^2, of the proton and neutron states in every core. So, in a first step, HF+BCS calculations [16, 17,18] were performed using the Skyrme III force [19] and usual pairing interaction with constant matrix elements (G_{0n} and G_{0p}) and standard cutoff. We used $G_{0n} = 15.5$, $G_{0p} = 13.6$ for ^{180,182}Os and $G_{0n} = 13.5$, $G_{0p} = 15.2$ for ^{182,184}Pt. These calculations have been performed with a constraint on the quadrupole moment in order to obtain the wave functions for several β deformation parameters. To ensure consistency, the same Skyrme III force has been used for the residual proton-neutron interaction, V_{pn}. In addition, the one-quasiparticle axial-rotor coupling model developed by Meyer *et al.* [20] has been used to follow the

Table 3. Energies for configurations expected at low energy (E < 1 MeV) in ^{182}Ir from zero-order estimation.

Configuration	K	E (keV)	Configuration	K	E (keV)
$\pi 1/2^-[541]\otimes\nu 1/2^-[521]$	1^+, 0^+	0	$\pi 1/2^-[541]\otimes\nu 9/2^+[624]$	4^-, 5^-	176
$\pi 1/2^-[541]\otimes\nu 7/2^-[514]$	4^+, 3^+	42	$\pi 3/2^+[402]\otimes\nu 1/2^-[521]$	2^-, 1^-	303
$\pi 1/2^-[541]\otimes\nu 5/2^-[512]$	2^+, 3^+	358	$\pi 5/2^+[402]\otimes\nu 1/2^-[521]$	2^-, 3^-	327
$\pi 1/2^-[541]\otimes\nu 7/2^-[503]$	3^+, 4^+	398	$\pi 3/2^+[402]\otimes\nu 7/2^-[514]$	5^-, 2^-	345
$\pi 3/2^+[402]\otimes\nu 9/2^+[624]$	3^+, 6^+	479	$\pi 1/2^-[541]\otimes\nu 7/2^+[633]$	3^-, 4^-	358
$\pi 3/2^-[532]\otimes\nu 1/2^-[521]$	2^+, 1^+	486	$\pi 1/2^+[400]\otimes\nu 1/2^-[521]$	0^-, 1^-	361
$\pi 5/2^+[402]\otimes\nu 9/2^+[624]$	7^+, 2^+	504	$\pi 5/2^+[402]\otimes\nu 7/2^-[514]$	1^-, 6^-	369
$\pi 9/2^-[514]\otimes\nu 1/2^-[521]$	4^+, 5^+	506	$\pi 1/2^+[400]\otimes\nu 7/2^-[514]$	3^-, 4^-	403
$\pi 3/2^-[532]\otimes\nu 7/2^-[514]$	5^+, 2^+	528	$\pi 3/2^+[402]\otimes\nu 5/2^-[512]$	1^-, 4^-	661
$\pi 1/2^+[400]\otimes\nu 9/2^+[624]$	5^+, 4^+	537	$\pi 3/2^-[532]\otimes\nu 9/2^+[624]$	3^-, 6^-	662
$\pi 9/2^-[514]\otimes\nu 7/2^-[514]$	1^+, 8^+	548	$\pi 9/2^-[514]\otimes\nu 9/2^+[624]$	9^-, 0^-	682
$\pi 3/2^+[402]\otimes\nu 7/2^+[633]$	2^+, 5^+	661	$\pi 5/2^+[402]\otimes\nu 5/2^-[512]$	5^-, 0^-	685
$\pi 5/2^+[402]\otimes\nu 7/2^+[633]$	6^+, 1^+	685	$\pi 3/2^+[402]\otimes\nu 7/2^-[503]$	2^-, 5^-	702
$\pi 1/2^+[400]\otimes\nu 7/2^+[633]$	4^+, 3^+	719	$\pi 1/2^+[400]\otimes\nu 5/2^-[512]$	3^-, 2^-	719
$\pi 3/2^-[532]\otimes\nu 5/2^-[512]$	1^+, 4^+	844	$\pi 5/2^+[402]\otimes\nu 7/2^-[503]$	6^-, 1^-	726
$\pi 9/2^-[514]\otimes\nu 5/2^-[512]$	7^+, 2^+	864	$\pi 3/2^-[532]\otimes\nu 7/2^+[633]$	2^-, 5^-	844
$\pi 3/2^-[532]\otimes\nu 7/2^-[503]$	2^+, 5^+	884	$\pi 9/2^-[514]\otimes\nu 7/2^+[633]$	8^-, 1^-	864
$\pi 9/2^-[514]\otimes\nu 7/2^-[503]$	8^+, 1^+	904	$\pi 1/2^+[400]\otimes\nu 7/2^-[503]$	4^-, 3^-	759
$\pi 1/2^-[541]\otimes\nu 1/2^-[510]$	0^+, 1^+		$\pi 3/2^+[402]\otimes\nu 1/2^-[510]$	1^-, 2^-	
$\pi 3/2^-[532]\otimes\nu 1/2^-[510]$	1^+, 2^+		$\pi 5/2^+[402]\otimes\nu 1/2^-[510]$	3^-, 2^-	
$\pi 1/2^-[541]\otimes\nu 3/2^-[512]$	2^+, 1^+		$\pi 3/2^+[402]\otimes\nu 3/2^-[512]$	3^-, 0^-	
$\pi 3/2^-[532]\otimes\nu 3/2^-[512]$	3^+, 0^+		$\pi 5/2^+[402]\otimes\nu 3/2^-[512]$	1^-, 4^-	

evolution of the neutron- and proton-state energies with the β deformation parameter.

4.2 Results from one-quasiparticle axial-rotor coupling model.

The results of the calculations performed using the Os cores are compared in fig. 5 (a) with the proton-state energies known in the ^{181,183}Ir nuclei [1,2,21,22,23,24,25, 26,27,28,29] and, in fig. 6 (a) with the neutron-state energies of ^{181}Os [30,31,32,33,34]. The results obtained using the Pt cores are compared with the particle-state energies in the ^{181,183}Ir nuclei for the protons and in the ^{183}Pt nucleus [35,36] for the neutrons in figs. 5 (b) and 6 (b) respectively. In figs. 5 and 6, the calculated $\pi 5/2^-$ $1/2^-[541]$ and $\nu 1/2^-[521]$ states have arbitrarily been drawn at zero energy because these states are the ground states in the odd-A nuclei, ^{181,183}Ir and ^{181}Os, ^{183}Pt, respectively. For the proton states, in all cases the $5/2^+[402]$ energy is badly reproduced by the calculations; it is about 600 keV too small from the Os cores and too large from the Pt cores at the expected deformation (see fig. 5). The $9/2^-[514]$ state is also calculated too high in energy from the Pt cores. The energies of the $3/2^+[402]$, $1/2^+[400]$ and $11/2^-[505]$ states are decreasing as the deformation decreases. The best agreement for the energy distance between the $3/2^+[402]$ and $5/2^-$ $1/2^-[541]$ states is obtained for $\beta \geq 0.24$ from the Pt cores and for $\beta \approx 0.214$ from the Os cores whereas the deformation deduced from laser spectroscopy measurements is $\beta = 0.207$ for the ^{183}Ir nucleus. Therefore,

Table 4. Occupation probabilities of proton and neutron states in the ^{180,182}Os and ^{182,184}Pt cores.

Core	^{180}Os	^{182}Os	^{182}Pt	^{184}Pt
β	0.214	0.214	0.214	0.214
p-state	v^2	v^2	v^2	v^2
$1/2^-[541]$	0.047	0.04	0.41	0.42
$3/2^-[532]$	0.019	0.02	0.13	0.17
$3/2^+[402]$	0.023	0.02	0.22	0.203
$1/2^+[400]$	0.015	0.01	0.13	0.12
$5/2^+[402]$	0.92	0.92	0.93	0.93
$9/2^-[514]$	0.97	0.98	0.95	0.96
$11/2^-[505]$	0.016	0.01	0.18	0.15
n-state	v^2	v^2	v^2	v^2
$1/2^-[521]$	0.76	0.93	0.73	0.92
$7/2^-[514]$	0.82	0.95	0.84	0.95
$5/2^-[512]$	0.72	0.92	0.71	0.9
$9/2^+[624]$	0.19	0.33	0.17	0.33
$7/2^+[633]$	0.72	0.91	0.69	0.9
$1/2^-[510]$	0.035	0.03	0.03	0.03
$3/2^-[512]$	0.033	0.03	0.03	0.03
$7/2^-[503]$		0.01		0.02
$9/2^-[505]$				0.02

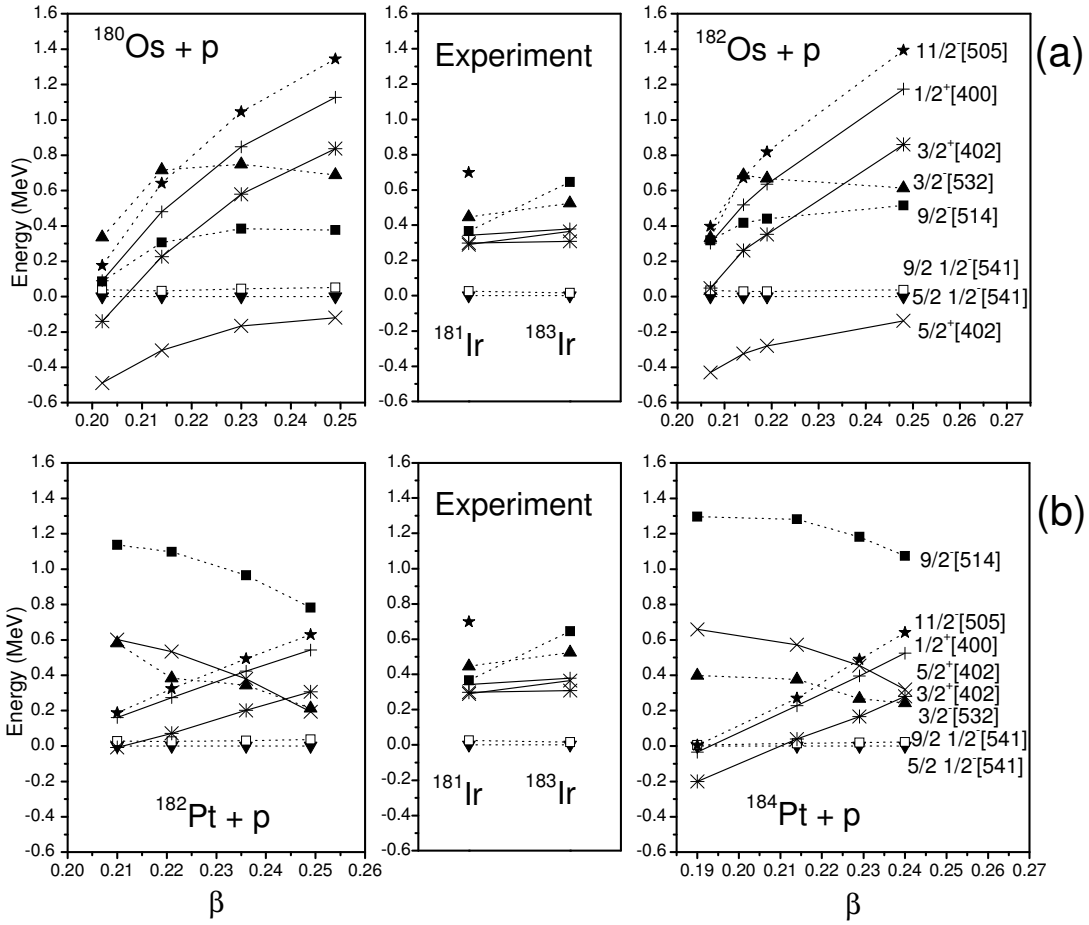

Fig. 5. Energy evolution of the proton states calculated using: (a) Os cores and (b) Pt cores compared with the experimental states observed in ^{181,183}Ir.

the proton states are generally better reproduced by the calculations performed using the Os cores with a deformation parameter $\beta \approx 0.214$. However, in this case, the $3/2^-[532]$ state is calculated too high in energy, about 200 keV. The occupation probabilities, v^2, have been reported in table 4 for the proton and neutron states in the four cores. The v^2 values are directly related to the state position above or below the Fermi level. For an occupied state, v^2 is close to 1 whereas for an almost empty state v^2 is small, $v^2 << 0.5$. We can see that, except for $5/2^+[402]$ and $9/2^-[514]$ orbitals having $v^2 \approx 1$ in all cores, $v^2 << 0.5$ for the proton states. This means that to add a proton to the $_{76}$Os cores is more suitable than to remove it from the $_{78}$Pt cores to well represent the proton states in the $_{77}$Ir nuclei close to A = 182. It is worth noting that the $5/2^+[402]$ and $9/2^-[514]$ states calculated using the Os cores, that have v^2 close to 1, indeed correspond to states in $_{75}$Re. For the neutron states, the results of the calculations are very similar for all cores: i) the $7/2^-[503]$ state energy is overestimated, ii) the $7/2^-[503]$, $9/2^-[505]$ and $5/2^+[642]$ state energies are increasing with β, iii) the $5/2^-[512]$ and $7/2^-[514]$ state energies are increasing as β decreases, iv) the $7/2^-[514]$ state is above the $5/2^-[512]$ state contrary to the experimental data. The main difference concerns the $i_{13/2}$ sub-shell : the $7/2^+[633]$ state is above the $9/2^+[624]$ state for the calculations performed using the ^{182}Os and ^{184}Pt cores whereas it is below it for the calculations with the ^{180}Os and ^{182}Pt cores. In this latter case its bandhead is 9/2, 11/2 or 13/2 instead of 7/2 (see figs. 6 (a) and (b)). This relative position change of the $7/2^+[633]$ and $9/2^+[624]$ states strongly suggests that the coupled states involving these two neutron states should be very close in energy in the ^{182}Ir nucleus. The v^2 values of the neutron states are very various (see table 4). It is actually impossible to choose a priori only one of the two Os cores. Therefore, this led us to perform the calculations for ^{182}Ir with both the Os cores.

4.3 Two-quasiparticle axial-rotor calculations.

From the facts discussed in the above section, we chose to perform the calculations, including the V_{pn} interaction, using both the ^{180,182}Os cores with a deformation $\beta = 0.214$. The Hamiltonian diagonalization was performed in the following proton and neutron quasiparticle space:
π: $1/2^-[541]$, $3/2^-[532]$, $3/2^+[402]$, and $1/2^+[400]$
ν: $1/2^-[521]$, $7/2^-[514]$, $5/2^-[512]$, $9/2^+[624]$, $7/2^+[633]$, and $7/2^-[503]$.

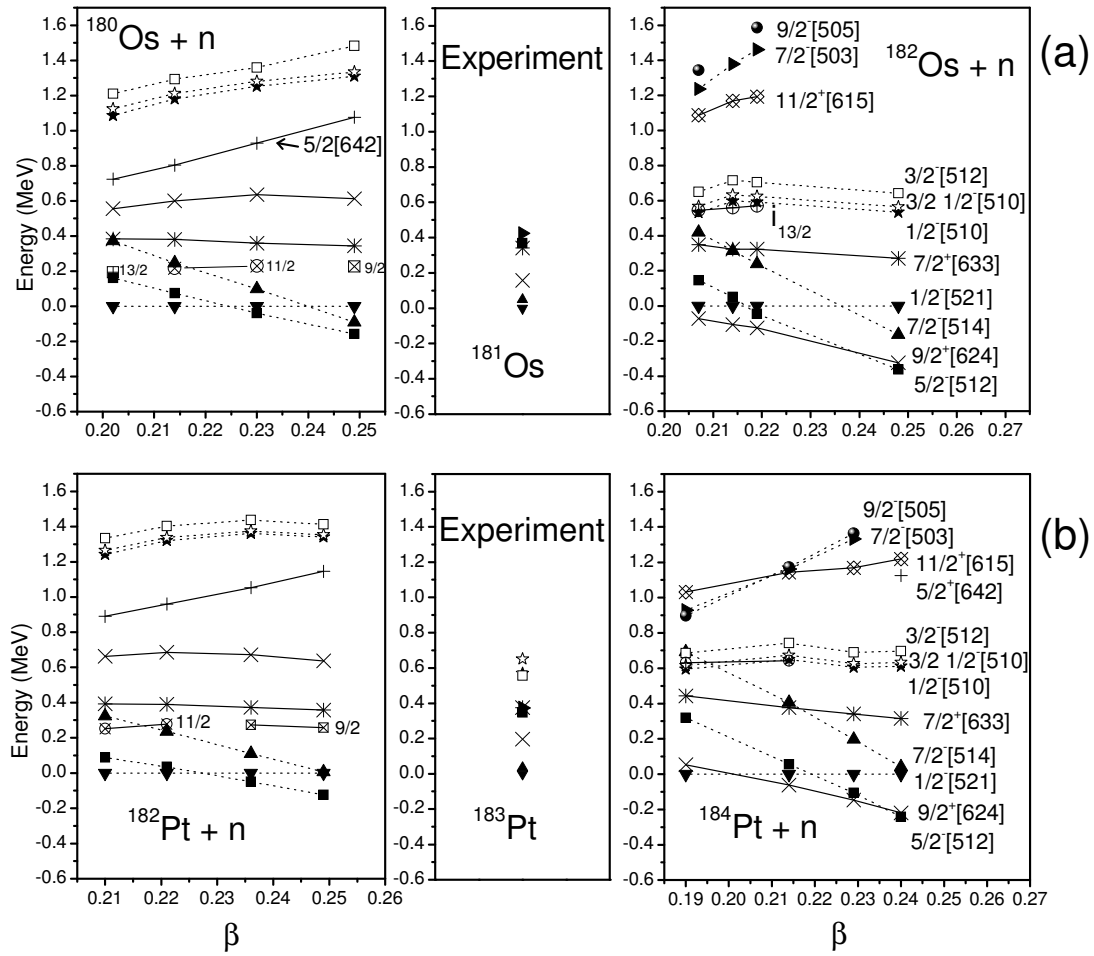

Fig. 6. Same as fig. 4 but for neutron states compared with experimental states of: (a) ^{181}Os and (b) ^{183}Pt.

The bandhead energies of the coupled states depend upon the core used to perform the calculations. They are shown for the ^{180}Os core in fig. 7, as an example. However, inside a given configuration the predictions obtained with both cores are very similar, even for the coupled states involving the $7/2^+[633]$ and $9/2^+[624]$ states. Therefore, in what follows, we shall compare only the theoretical results obtained using the ^{180}Os core with the experimental data.

4.3.1 $\pi 1/2^-[541] \otimes \nu 1/2^-[521]$ and $\pi 3/2^-[532] \otimes \nu 1/2^-[521]$ configurations.

The $\pi 1/2^-[541] \otimes \nu 1/2^-[521]$ configuration with $K = 1$ has been assigned to the ^{182}Ir ground state in ref. [1]. The 25.7 keV $E2$ transition observed in the present work and the nuclear moments measured by laser spectroscopy [3] unambiguously confirm this assumption. The calculations show that the wave functions of the states built on this ground state configuration with $K = 1$ have large admixtures with the partner $K = 0$ and also admixtures with the two partners $K = 1$ and $K = 2$ of the $\pi 3/2^-[532] \otimes \nu 1/2^-[521]$ configuration in spite of the rather large energy distance predicted and observed between the $\pi 1/2^-[541]$ and $\pi 3/2^-[532]$ states of $h_{9/2}$ parentage (see fig. 5). The main components of the wave functions of some of the states corresponding to these configurations are given in table 5. It is very clear that the 3^+ ground state and the levels: 5^+ located at 25.7 keV, 2^+ at 74.8 keV and 4^+ at 95.1 keV which decay without delay to the ground state, correspond to the first states of table 5 that have a main $K = 1$ component. The $1{,}2^+$ level at 87.4 keV is very likely the 1^+ state of the same configuration. The 5^+, 7^+, 9^+, 11^+ ... levels of the doubly-decoupled ground-state band observed in the in-beam experiment [2] have obviously the same configuration. The 4^+, 6^+, 8^+, 10^+, 12^+ ... levels of the unfavored band have been observed more recently in an in-beam experiment [11]. This band is built on a 4^+ state at 68.1 keV above the 5^+ level at 25.7 keV. The 4^+ state we observed in this work is at 69.3 keV above the same 5^+ level. We believe that the 4^+ level observed in ref. [11] is the 4^+ level established in this work in spite of their 1.2 keV energy difference. The experimental levels are compared, in fig. 8, with the predicted states for the partners $K = 1$ and $K = 0$ of the $\pi 1/2^-[541] \otimes \nu 1/2^-[521]$ configuration. The states with main $K = 0$ component are tagged by an open circle. We can see in fig. 8 that these latter low-spin states are predicted at rather low energy,

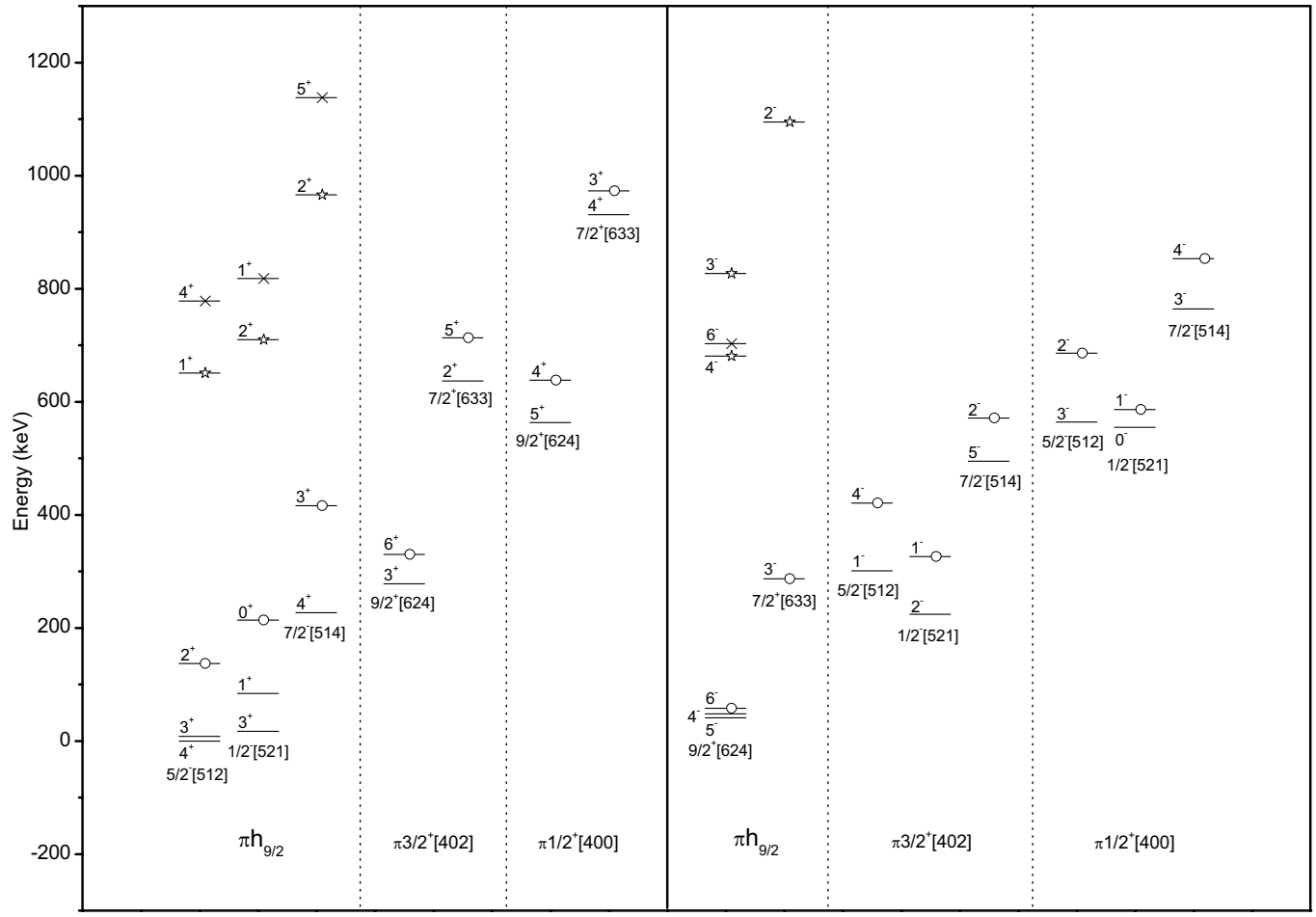

Fig. 7. Bandhead spectrum calculated using the ^{180}Os core at $\beta = 0.214$ deformation. $h_{9/2}$ implies the $1/2^-[541]$ and $3/2^-[532]$ proton states. The favored (unfavored) bandheads are tagged by a star (cross) for the coupled states involving the $3/2^-[532]$ state. The unfavored bandheads are marked by an open circle in the other cases. When the $I = K$ state of the rotational band is not located at the lowest energy, the state located at the lowest energy in that band is also shown.

which suggests that we should observe them. In the Au $\rightarrow$ Pt and Ir $\rightarrow$ Os β decays, the $\nu 3/2^-$ $1/2^-[521]$ state is fed by the $\pi 5/2^-$ $1/2^-[541]$ one [37]. Therefore, the large feeding in the β decay of the 1^+ level located at 211.0 keV suggests that it could be the 1^+ state of the $K = 0$ partner. There is no level with possible spin $I = 0$ observed below this 1^+ state. On the other hand, there are two levels with unique spin assignment 2^+ located above the 1^+ state at 211.0 keV. The first one, at 259.7 keV decays towards the $(1)^+$ and 3^+ states of the ground-state configuration and also to the 4^+ level located at 88.8 keV whereas the second, at 283.9 keV decays only to $(1)^+$ and 3^+ states of the ground state configuration. This suggests that the second state at 283.9 keV is the best candidate to be the 2^+ state of the $K = 0$ $\pi 1/2^-[541] \otimes \nu 1/2^-[521]$ configuration. The 2, 3 or 4^+ level at 341.5 keV could be the 3^+ state of this configuration since it de-excites only to the 4^+ and 2^+ states of the ground-state configuration. Thus, the configuration $\pi 1/2^-[541] \otimes \nu 1/2^-[521]$ with mainly $K = 0$ is attributed to the 1^+ level located at 211.0 keV, the 2^+ level at 283.9 keV and the $(3)^+$ level at 341.5 keV in fig. 8. However, it is worth noting that it is rather difficult to understand why the 1^+ state at 211.0 keV is strongly fed whereas the $(1)^+$ state at 87.4 keV is not. The character $K = 0$ could be the reason of this favored feeding, which would suggest that the admixtures in the wave functions are overestimated. However, the $K = 0{,}1$ mixture in the wave function of the 3^+ ground state was expected from the feedings of the 2^+ and 4^+ levels of the ground state band of ^{182}Os which are similar to those observed in the ^{174}Ta $\rightarrow$ ^{174}Yb decay [38]. Furthermore, it is in very good agreement with the quadrupole moment measured by laser spectroscopy [3]. Thus, this fact remains unexplained. The two first states of every partners $K = 2$ and $K = 1$ of the π $3/2^-[532] \otimes \nu 1/2^-[521]$ configuration are also drawn in fig. 8 though they are predicted at rather high energy and could not be identified.

Table 5. Main components in % of the wave functions calculated for the first states of the $\pi 1/2^-[541] \otimes \nu 1/2^-[521]$ and $\pi 3/2^-[532] \otimes \nu 1/2^-[521]$ configurations, using the ^{180}Os core with $\beta = 0.214$ deformation parameter. The experimental energies of the levels for which an assignment is proposed are given in the last column.

I^π	E_{th} (keV)	$\pi\frac{1}{2}^-[541]\otimes\nu\frac{1}{2}^-[521]$ $K=0$	$K=1$	$\pi\frac{3}{2}^-[532]\otimes\nu\frac{1}{2}^-[521]$ $K=1$	$K=2$	E_{exp} (keV)
3^+	0	33	40			0
2^+	33	36	52	8.3		74.8
5^+	47	42	47		7.7	25.7
1^+	67	37	62			(87.4)
4^+	72	37	47	9.4	5.5	95.1
7^+	227	42	44		8.9	171
6^+	247	37	46	10	7.1	(238)
9^+	525	41	43		9.5	439
8^+	541	37	44	10	8.1	(504)
11^+	915	41	43	5.5	9.7	807
10^+	929	37	44	10	8.7	(878)
12^+	1385	37	44	10	9.1	(1336)
0^+	197	100				
1^+	264	58	30	12		211.0
2^+	379	54	35		9.7	(283.9)
3^+	442	39	29	23	8.0	341.5
4^+	555	37	26	11	26	
2^+	693		5.2	8.6	68	
3^+	787			17	65	
1^+	801	5.0	7.5	87		
2^+	889	5.0	5.3	81	7.7	

4.3.2 $\pi 1/2^-[541] \otimes \nu 7/2^-[514]$ and $\pi 3/2^-[532] \otimes \nu 7/2^-[514]$ configurations.

The bandhead of the $\pi 1/2^-[541] \otimes \nu 7/2^-[514]$ configuration is expected at 42 keV from the zero-order estimation (see table 3). The properties of the rotational band built on a 5^+ state that is observed in in-beam experiments [2, 11] and also in the present work above the 45.3 keV transition, allows the identification of the 5^+ state at 71.0 keV as the bandhead of the $K = 4$ partner of the $\pi 1/2^-[541] \otimes \nu 7/2^-[514]$ configuration. The calculations predict a 4^+ as the bandhead and a 5^+ at 11 keV above it while the 4^+ is observed at 17.8 keV above the 5^+ level. The 3^+ level located at 190.4 keV that decays only towards the 4^+ state at 88.8 keV is very likely the $K = 3$ partner of the same configuration. The 2^+ level at 377.2 keV de-excites only to this 3^+ level. It could be the favored $K = 2$ partner of the $\pi 3/2^-[532] \otimes \nu 7/2^-[514]$ configuration though it is much lower in energy than expected from the calculations. These experimental levels and the first members of the rotational band established in refs. [2,11] are compared with the results of the calculations in fig. 9. The main components of the wave functions of these states are given in table 6. There are large admixtures in the wave functions especially between the $K = 3$ and 4 partners of the $\pi 1/2^-[541] \otimes \nu 7/2^-[514]$ configuration due to the $\Delta K = 1$ value that implies important Coriolis effects. We can see that the admixtures with the $\pi\ 3/2^-[532] \otimes \nu 7/2^-[514]$ configuration also exist but are weaker. In addition to this, no admixture exists with the $\pi 1/2^-[541] \otimes \nu 5/2^-[512]$ and $\pi\ 3/2^-[532] \otimes \nu 5/2^-[512]$ configurations excepted for the 3^+ state predicted at 189 keV that has 10% on the $K = 2$ and 17% on the $K = 3$ partners of the $\pi 1/2^-[541] \otimes \nu 5/2^-[512]$ configuration. This lack of admixture is surprising because the energy distance calculated between the $\pi 1/2^-[541] \otimes \nu 7/2^-[514]$ and $\pi 1/2^-[541] \otimes \nu 5/2^-[512]$ configurations is only 227 keV (see fig. 7). The first state of the $\pi 1/2^-[541] \otimes \nu 7/2^-[514]$ configuration is located at higher energy than expected from table 3, which is not surprising since the energy of the $\nu 7/2^-[514]$ state increases as deformation decreases (see fig. 6).

4.3.3 Negative-parity states.

The first negative-parity level is observed at 152.3 keV, it has $I = 1$ or 2 as spin value and de-excites mainly to the 2^+ state of the $K = 1$ $\pi 1/2^-[541] \otimes \nu 1/2^-[521]$ configuration. The first candidates for $I = 2$ correspond to the $\pi\ 3/2^+[402] \otimes \nu 1/2^-[521]$ and $\pi\ 5/2^+[402] \otimes \nu 1/2^-[521]$ configurations from the zero-order estimation and that for $I = 1$ to the $\pi\ 5/2^+[402] \otimes \nu 7/2^-[514]$ configuration (see table 3). The 2^- state of the $K = 2$ $\pi 3/2^+[402] \otimes \nu 1/2^-[521]$ configuration is the best candidate because it is expected to be located at the lowest energy. In this case the 77.4 keV transition corresponds to a proton $3/2^+[402] \rightarrow 1/2^-[541]$ transition. Such an $E1$ $3/2^+[402] \rightarrow 5/2$

Table 6. Same as table 5 but for states of the $\pi 1/2^-[541] \otimes \nu 7/2^-[514]$ and $\pi 3/2^-[532] \otimes \nu 7/2^-[514]$ configurations.

I^π	$E_{theo.}$ (keV)	$\pi\frac{1}{2}^-[541]\otimes\nu\frac{7}{2}^-[514]$ $K=3$	$K=4$	$\pi\frac{3}{2}^-[532]\otimes\nu\frac{7}{2}^-[514]$ $K=2$	$K=5$	$E_{exp.}$ (keV)
4^+	0	41	53			88.8
5^+	11	39	52			71.0
6^+	62	36	50		8.5	110.0
7^+	163	35	47		9.6	185.7
8^+	300	34	45		10	292.2
9^+	466	34	44		10	425.8
10^+	657	33	43	5.0	10	591.0
11^+	868	33	42	5.2	10	776.7
12^+	1097	33	41	5.3	10	985.7
3^+	189	64				190.4
4^+	382	39	31	7.6		
2^+	739			99		377.2
3^+	875	5.9		89		
5^+	911			11	52	

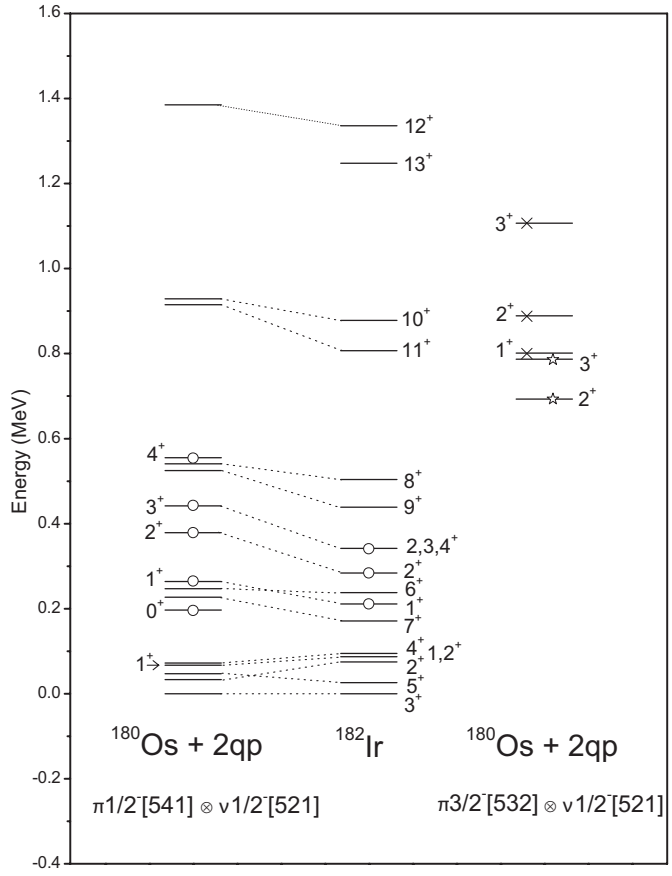

Fig. 8. Comparison of the observed states with the predicted ones for the $\pi 1/2^-[541] \otimes \nu 1/2^-[521]$ and $\pi 3/2^-[532] \otimes \nu 1/2^-[521]$ configurations, calculated using the ^{180}Os core at $\beta = 0.214$ deformation. States mainly corresponding to the unfavored partner of the first configuration are tagged by an open circle, those of the second configuration by a cross. The states of the favored partner of the second configuration are marked by a star.

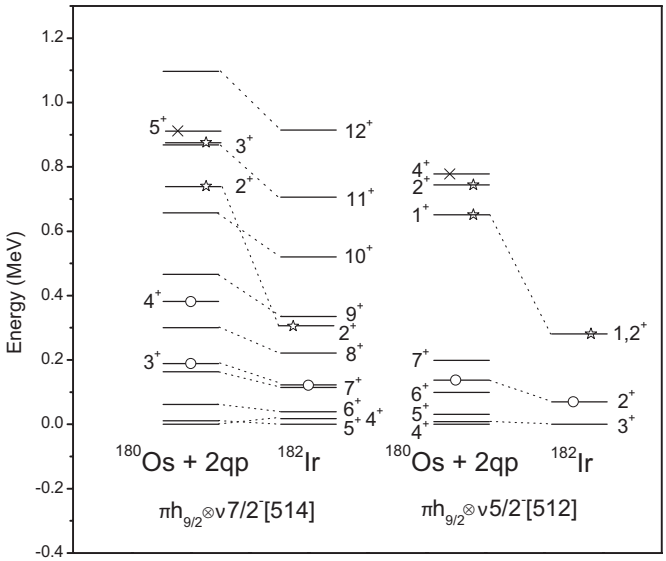

Fig. 9. Same as fig. 8 but for the $\pi 1/2^-[541] \otimes \nu 7/2^-[514]$ and $\pi 3/2^-[532] \otimes 7/2^-[514]$ configurations.

$1/2^-[541]$ transition is observed in ^{185}Ir [39] and has a hindrance factor $Fw = 1.8 \times 10^5$, if the 77.4 keV transition has similar hindrance factor, then the half-life of the 152.3 keV level would be $T_{1/2} \approx 30$ ns. It is clear that for the two other configurations the $T_{1/2}$ value would be longer. The 152.3 keV level is a short half-life isomeric state but, unfortunately, its $T_{1/2}$ value could not be exactly determined in the present work. So, it is only the level-energy argument that allows us to attribute the $K = 2$ $\pi 3/2^+[402] \otimes \nu 1/2^-[521]$ configuration to the 152.3 keV level. The level at 199.9 keV that has $I = 0$, 1, 2, or 3 as spin value and de-excites only to the 152.3 keV level is, then, either the rotational state $I = 3$ built on the 2^- state or the $K = 1$ partner of the same $\pi 3/2^+[402]$

$\otimes$ $\nu 1/2^-[521]$ configuration. The 152.5 keV level has $I = 4$ and decays mainly towards the 5^+ state, bandhead of the $\pi 1/2^-[541] \otimes \nu 7/2^-[514]$ configuration. This state could be the favored $K = 4$ bandhead of the $\pi 1/2^-[541] \otimes \nu 9/2^+[624]$ configuration or the unfavored $K = 4$ bandhead of the $\pi 1/2^-[541] \otimes \nu 7/2^+[633]$ configuration from table 3. A negative-parity rotational band built on a 6^- level [2] or a 5^- level [11] that de-excites by a 105.7 keV transition to the 5^+ state of the $\pi 1/2^-[541] \otimes \nu 7/2^-[514]$ configuration has been observed in in-beam experiments. The 81.5 keV $E1$ transition that de-excites the 4^- level at 152.5 keV in the present work was also observed in the in-beam experiments but the transition $5^- \rightarrow 4^-$ was not. The calculations performed with the ^{180}Os core predict that the $\pi 1/2^-[541] \otimes \nu 9/2^+[624]$ configuration is located at the lowest energy according to table 3. All of this suggests that the 4^- level at 152.5 keV and the 5^- bandhead of the rotational band would have the $\pi 1/2^-[541] \otimes \nu 9/2^+[624]$ configuration. Moreover, this configuration has been proposed in ref. [2] for the rotational band from its properties but the spin values must be changed by one unit to take into account the signature inversion phenomenon present in this structure [40]. In this work the level at 152.5 keV is clearly a state with a long half-life, in the in-beam experiment the half-life has been estimated $T_{1/2} > 1\mu$s [11]. This value corresponds to a hindrance factor Fw $> 5 \times 10^6$ for the 81.5 keV $E1$ transition, which is compatible with the hindrance factor Fw $= 2.5 \times 10^6$ found for the $E1$ $9/2^+[624] \rightarrow 7/2^-[514]$ transition in ^{181}Os [41]. This fact supports also the attribution of the $\pi 1/2^-[541] \otimes \nu 9/2^+[624]$ configuration to the 4^- level at 152.5 keV. The 3^- level located at 174.5 keV decays only towards the 4^- level at 152.5 keV and it is very likely the favored $K = 3$ partner of the $\pi 1/2^-[541] \otimes \nu 7/2^+[633]$ configuration. In the calculations there is an inversion of the favored and unfavored states relatively to the Gallagher and Moskowski rule. So the 3^- state becomes the unfavored partner of the configuration but the wave function of the 5^- of the favored $K = 4$ partner has very large admixtures (see table 7). The possible configurations for the two 2^- levels located at 321.1 and 345.9 keV are the following from table 3:
- favored $K = 2$ $\pi 5/2^+[402] \otimes \nu 1/2^-[521]$,
- unfavored $K = 2$ $\pi 3/2^+[402] \otimes \nu 7/2^-[514]$,
- favored $K = 2$ $\pi 3/2^+[402] \otimes \nu 7/2^-[503]$,
- unfavored $K = 2$ $\pi 1/2^+[400] \otimes \nu 5/2^-[512]$,
- favored $K = 2$ $\pi 3/2^-[532] \otimes \nu 7/2^+[633]$.

The observed 2^- levels do not de-excite to the states with the $\pi 1/2^-[541] \otimes \nu 7/2^-[514]$ configuration or $\pi 3/2^-[532] \otimes \nu 7/2^-[514]$ configuration, which eliminates the second possible configuration. The 2^- level at 321.1 keV decays to:
- the 3^- level at 174.5 keV of main $K = 3$ $\pi 1/2^-[541] \otimes \nu 7/2^+[633]$ configuration,
- the $(2)^-$ level at 152.3 keV of main $K = 2$ $\pi 3/2^+[402] \otimes \nu 1/2^-[521]$ configuration, and
- the 1^+ level at 211.0 keV of main $K = 0$ $\pi 1/2^-[541] \otimes \nu 1/2^-[521]$ configuration.

The 2^- level at 345.9 keV de-excites to:
- the 3^- level at 174.5 keV of main $K = 3$ $\pi 1/2^-[541] \otimes \nu 7/2^+[633]$ configuration and
- the 2^- level at 321.1 keV.

From the decay modes, the 2^- level at 321.1 keV has more likely the favored $K = 2$ π $5/2^+[402] \otimes \nu 1/2^-[521]$ configuration, the 2^- level at 345.9 keV the favored $K = 2$ π $3/2^-[532] \otimes \nu 7/2^+[633]$ configuration and the link between the two states is then due to large admixtures in the wave functions of these states because of their small energy difference. This large mixing would be also responsible for the decay of the 321.1 keV level towards the 3^- level at 174.5keV. Unfortunately, this cannot be confirmed by the calculations since the energy of the $\pi 5/2^+[402]$ state is very badly reproduced (see fig. 5). The levels of the probable $\pi 1/2^-[541] \otimes \nu 9/2^+[624]$ and $\pi 3/2^-[532] \otimes \nu 7/2^+[633]$ configurations are compared to the predictions in fig. 10 and the main components of the corresponding wave functions are reported in table 7. We can see that the main component of the members of the rotational band has $K = 5$ when the spin value is $I > 5$. For the 3^- state, there is a large admixture of the $\pi 1/2^-[541] \otimes \nu 7/2^+[633]$ configuration with the $\pi 3/2^-[532] \otimes \nu 9/2^+[624]$ configuration. The 2^- level of $K = 2$ π $3/2^-[532] \otimes \nu 7/2^+[633]$ configuration is predicted at rather high energy (see fig. 10). We can note that the calculated energy spectrum for the $\pi 1/2^-[541] \otimes \nu 9/2^+[624]$ configuration is more compressed than the experimental one contrary to those obtained for the two previous configurations (see figs. 8, 9, and 10). Such a too compressed energy spectrum was also obtained for ^{184}Ir, calculated using the ^{184}Pt core at $\beta = 0.214$ (see ref. [42]). Furthermore, the energy spectrum of the rotational band is predicted to be more regular than the observed one, which is similar to the case in ^{184}Au [43].

4.3.4 Other states.

The 3^+ level at 382.2 keV de-excites to the 3^+, 2^+ and 4^+ states of the mainly $K = 1$ $\pi 1/2^-[541] \otimes \nu 1/2^-[521]$ configuration and to the 4^- state of the $\pi 1/2^-[541] \otimes \nu 9/2^+[624]$ configuration. The possible configurations for this level are the following from table 3:
- the unfavored $K = 3$ $\pi 1/2^-[541] \otimes \nu 5/2^-[512]$,
- the favored $K = 3$ $\pi 1/2^-[541] \otimes \nu 7/2^-[503]$,
- the favored $K = 3$ π $3/2^+[402] \otimes \nu 9/2^+[624]$.

For the $\pi 1/2^-[541] \otimes \nu 5/2^-[512]$ configuration the theoretical calculations predict the $K = 3$ partner as favored state contrary to the Gallagher and Moskowski rule (see fig. 7). So, the best candidate for the 3^+ level at 382.2 keV is this $K = 3$ $\pi 1/2^-[541] \otimes \nu 5/2^-[512]$ configuration predicted as the favored coupled state and expected at the lowest energy from the zero-order estimation. This assignment, involving the $\nu 5/2^-[512]$ orbital, allows us to understand the prompt decaying of the 382.2 keV level to the coupled states implying both the $\nu 1/2^-[521]$ and $\nu 9/2^+[624]$ states. The 2^+ level at 452.5 keV that decays to the 3^+ level at 382.2 keV, 3^- level of main $K = 3$ $\pi 1/2^-[541] \otimes \nu 7/2^+[633]$ configuration and 3^+ state of $\pi 1/2^-[541] \otimes \nu 7/2^-[514]$ configuration is very likely the

Table 7. Same as table 5 but for states of the $\pi 1/2^-[541] \otimes \nu 9/2^+[624]$, $\pi 3/2^-[532] \otimes \nu 9/2^+[624]$, $\pi 1/2^-[541] \otimes \nu 7/2^+[633]$, and $\pi 3/2^-[532] \otimes \nu 7/2^+[633]$ configurations.

I^π	$E_{theo.}$ (keV)	$\pi\frac{1}{2}^-[541]\otimes\nu\frac{9}{2}^+[624]$ $K=4$	$K=5$	$\pi\frac{3}{2}^-[532]\otimes\nu\frac{9}{2}^+[624]$ $K=3$	$K=6$	$\pi\frac{1}{2}^-[541]\otimes\nu\frac{7}{2}^+[633]$ $K=3$	$K=4$	$\pi\frac{3}{2}^-[532]\otimes\nu\frac{7}{2}^+[633]$ $K=2$	$K=5$	$E_{exp.}$ (keV)
5^-	0	44	43							176.7
4^-	7	71					25			152.5
6^-	10	35	46			8.7				211.7
7^-	39	30	43		5.7	11	5.6			290.9
8^-	94	27	39		7.1	13	8.7			371.1
9^-	178	25	37		7.9	14	11			544.2
10^-	293	24	34		8.2	14	12			656.8
11^-	436	23	33		8.4	15	13			932
12^-	605	23	32		8.4	15	14			1063.5
3^-	246			41		59				174.5
4^-	315	5.4		21		65	7.8			
5^-	179	23	32	7.2			35			
3^-	786			43		29		28		
2^-	1054							90		345.9
3^-	1256			12		8.6		47		

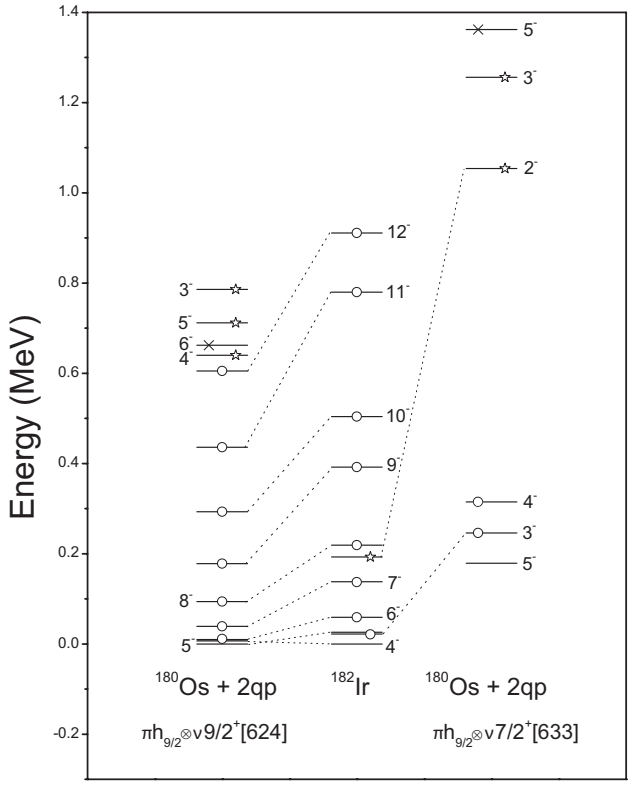

Fig. 10. Same as fig. 8 but for the $\pi 1/2^-[541] \otimes \nu 9/2^+[624]$, $\pi 3/2^-[532] \otimes \nu 9/2^+[624]$, $\pi 1/2^-[541] \otimes \nu 7/2^+[633]$, and $\pi 3/2^-[532] \otimes \nu 7/2^+[633]$ configurations. The open circles indicate the states of the unfavored partners of the configurations mainly involving the $\pi 1/2^-[541]$ state. For the configuration implying the $\pi 3/2^-[532]$ state, the levels of the favored partner are marked by a star, those of the unfavored partner by a cross.

$K = 2$ partner of the $\pi 1/2^-[541] \otimes \nu 5/2^-[512]$ configuration. The experimental levels are compared with calculated states of the $\pi 1/2^-[541] \otimes \nu 5/2^-[512]$ configuration in fig. 9. Two $1,2^+$ levels at 636.9 and 662.8 keV decay to states of the $\pi 1/2^-[541] \otimes \nu 1/2^-[521]$ configuration and to the 2^+ state of the $\pi 1/2^-[541] \otimes \nu 5/2^-[512]$ configuration. The level at 662.8 keV that decays mainly to the 2^+ state of the $\pi 1/2^-[541] \otimes \nu 5/2^-[512]$ configuration could have the $K = 1\ \pi\ 3/2^-[532] \otimes \nu 5/2^-[512]$ configuration.

Configurations are proposed for most of the states located below 700 keV. Three positive-parity low-spin states located at 194.3, 259.7 and 255.1 keV remains without identification. We have to recall that the $\pi 3/2^-[532]$ state is calculated at too high energy of about 200 keV from the Os cores but the coupled states involving the $\pi 3/2^-[532]$ state are systematically located at much lower energies than expected from the calculations. The coupled states with the $\pi 3/2^-[532]$ state are about 200 keV above the corresponding coupled states with the $\pi 1/2^-[541]$. Thus, one of the remaining states could have the $K = 2\ \pi 3/2^-[532] \otimes \nu 1/2^-[521]$ configuration. States corresponding to the $K = 1\ \pi 9/2^-[514] \otimes \nu 7/2^-[514]$ configuration could be also located at low energy. A calculation performed in configuration space including the $\pi 9/2^-[514]$ state leads indeed to low-energy levels for the $\pi 9/2^-[514] \otimes \nu 7/2^-[514]$ configuration. The decay modes of the three remaining states do not allow us to assign configurations to them. It is worth noting that the 1^+ level at 1002.5 keV, strongly fed in the β decay of ^{182}Pt, de-excites mainly towards the 2^- states located at 321.1 and 345.9 keV. It behaves in a similar manner to the most fed 1^+ states of ^{184,186}Au and ^{184}Ir that also decay mainly to negative-parity states with $I = 1, 2$ levels [43,44,45]. From table 3 the 1^+ levels expected at rather high energy could have the following configurations:

- unfavored $K = 1$ $\pi 5/2^+[402] \otimes \nu 7/2^+[633]$,
- unfavored $K = 1$ $\pi 9/2^-[514] \otimes \nu 7/2^-[503]$,
- unfavored $K = 1$ $\pi 1/2^-[541] \otimes \nu 1/2^-[510]$,
- unfavored $K = 1$ $\pi 1/2^-[541] \otimes \nu 3/2^-[512]$, or
- favored $K = 1$ $\pi 3/2^-[532] \otimes \nu 1/2^-[510]$.

The first configuration would allow us to explain the decay mainly to the 2^- levels at 321.1 and 345.9 keV for which we proposed $K = 2$ $\pi 5/2^+[402] \otimes \nu 1/2^-[521]$ and $K = 2$ $\pi 3/2^-[532] \otimes \nu 7/2^+[633]$ configurations with a large admixture. However, it is expected to be located at a too low energy from table 3. The $\nu 1/2^-[510]$ and $\nu 3/2^-[512]$ states were found around 600 keV in ^{183}Pt. For the configuration implying these neutron states it is very difficult to explain the observed decay mode. The unfavored $K = 1$ $\pi 9/2^-[514] \otimes \nu 7/2^-[503]$ configuration could be the best candidate. Indeed, the $\pi 9/2^-[514]$ is coming from the $h_{11/2}$ sub-shell, the $\nu 7/2^-[503]$ is arising from the $h_{9/2}$ sub-shell and a $\pi h_{11/2} \rightarrow \nu h_{9/2}$ transition is expected to be very favored. For such a configuration, it is also difficult to explain the favored decay mode. For states located at such energy, it is probable that the states correspond to a large admixture of different configurations resulting in no selective decay modes, which makes it difficult to assign a configuration.

4.4 Levels linked by the 34.0 keV transition in ^{178}Re.

This 34.0 keV transition could be the $5^+ \rightarrow 3^+$ transition linking the two first states of the band corresponding to the $\pi h_{9/2} \otimes \nu\ 1/2^-[521]$ configuration. Nevertheless, in the framework of the Cranking Model [46] the 34.0 keV energy is lower than the expected value for this transition in ^{178}Re. For the cases in which the $5^+ \rightarrow 3^+$ transition has been observed, we extracted the inertia and alignment parameters from the first three transitions of the band, beginning from the $7^+ \rightarrow 5^+$ transition, and we used these values to calculate the $5^+ \rightarrow 3^+$ transition energy, E^{calc}. As we show in table 8, we obtain a good agreement with the experimental values, E^{exp}, and always $E^{calc} < E^{exp}$. At variance with these results, for ^{178}Re [52] we obtain $E^{calc} = 53.1$ keV, which is rather high to fit in the present systematics.

Table 8. Experimental and calculated $5^+ \rightarrow 3^+$ transition energy for $\pi h_{9/2} \otimes \nu\ 1/2^-[521]$ bands.

Nucleus	E^{exp} (keV)	E^{calc} (keV)
^{170}Lu [47]	91.9	89.8
^{172}Lu [48]	80	74.6
^{172}Ta [49]	91.5	87.5
^{174}Ta [50]	77.0	73.4
^{176}Re [51]	76.2	70.9
^{182}Ir	25.7	22.6

5 Conclusions

Two experiments have been performed to measure internal-conversion electron and γ intensities as well as to obtain electron-γ coincidence relationships of transitions belonging mainly to the ^{182}Ir nucleus. This allowed the determination of the probable multipolarity of most of the observed transitions. The multipolarities, previously obtained from intensity balances in ref. [1] for five transitions, have been confirmed. Moreover, the multipolarities have been determined for 69 transitions and restricted for 9 other ones. These results led us to introduce small changes in the level scheme. Thus, four new levels have been added in the ^{182}Ir level scheme at 458.4, 615.2, 783.0 and 922.9 keV. The inversion of the 101.6 and 17.8 keV transitions in the observed cascade led us to change the energy of the intermediate level from 172.6 to 88.8 keV. Furthermore, the observation of the 25.7 keV $E2$ transition populating the ground state has confirmed the spin and parity values $I^\pi = 3^+$ that had been assumed in ref. [1] for the ^{182}Ir ground state. The determination of the multipolarities has also confirmed the spin and parity values $I^\pi = 4^-$ suggested in ref. [11] for the 152.5 keV level and allowed the attribution of unique spin and parity values for 16 other excited levels of the ^{182}Ir nucleus. Besides, a 34 keV $E2$ transition belonging very likely to ^{178}Re has been revealed by the high-resolution electron measurement. This transition could be the $5^+ \rightarrow 3^+$ transition of the $\pi 1/2^-[541] \otimes \nu 1/2^-[521]$ configuration. The comparison of the experimental levels established in ^{182}Ir with the states predicted using the semi-microscopic two-quasiparticle axial-rotor coupling model allows us to confirm the presence of the three configurations, $\pi h_{9/2} \otimes \nu 1/2^-[521]$, $\pi h_{9/2} \otimes \nu 7/2^-[514]$, and $\pi h_{9/2} \otimes \nu 9/2^+[624]$ previously suggested in refs. [1,2,11] and to attribute a configuration to most of the levels located below 700 keV in ^{182}Ir.

- The $\pi 1/2^-[541] \otimes \nu 1/2^-[521]$ configuration mainly $K = 1$ has been attributed to the 3^+ ground state, 5^+ at 25.7 keV, 2^+ at 74.8 keV, $(1)^+$ at 87.4 keV, 4^+ at 95.1 keV and to the corresponding high-spin levels of refs. [2,11].
- The $\pi 1/2^-[541] \otimes \nu 1/2^-[521]$ configuration mainly $K = 0$ has been proposed for the 1^+ at 211.0 keV, 2^+ at 283.9 keV and $(3)^+$ at 341.5 keV.
- The $\pi 1/2^-[541] \otimes \nu 7/2^-[514]$ configuration mainly $K = 4$ has been assigned to the 5^+ level at 71.0 keV, 4^+ at 88.8 keV and to the corresponding high-spin levels of refs. [2,11].
- The $\pi 1/2^-[541] \otimes \nu 7/2^-[514]$ configuration mainly $K = 3$ has been attributed to the 3^+ level at 190.4 keV.
- The $K = 2$ $\pi 3/2^-[532] \otimes \nu 7/2^-[514]$ configuration has been suggested for the 2^+ level located at 377.2 keV.
- The $\pi 3/2^+[402] \otimes \nu 1/2^-[521]$ configuration has been assigned to the 1, 2^- level lying at 152.3 keV as the partner

mainly $K = 2$ and to the level at 199.9 keV either as the $I = 3$ state of the $K = 2$ partner or as the unfavored partner $K = 1$.
- The $K = 2$ $\pi 5/2^+[402] \otimes \nu 1/2^-[521]$ configuration has been suggested for the 2^- level at 321.1 keV.
- The $\pi 1/2^-[541] \otimes \nu 9/2^+[624]$ configuration has been attributed to the 4^- level at 152.5 keV and the negative-parity band of ref. [11].
- The $K = 3$ $\pi 1/2^-[541] \otimes \nu 7/2^+[633]$ configuration has been attributed to the 3^- level at 174.5 keV.
- The $K = 2$ $\pi 3/2^-[532] \otimes \nu 7/2^+[633]$ configuration has been proposed for the 2^- level at 345.9 keV.
- The $\pi 1/2^-[541] \otimes \nu 5/2^-[512]$ configuration has been attributed to the 3^+ at 382.2 keV and 2^+ at 452.5 keV as the two $K = 3$ and $K = 2$ partners.
- The $\pi 3/2^-[532] \otimes \nu 5/2^-[512]$ configuration has been suggested for the 1, 2^+ level at 662.8 keV.

A rather good agreement is obtained between the observed level energies and the calculated ones especially for the positive-parity states. The calculations have shown that there exists important Coriolis effects for the coupled states involving the $\pi 1/2^-[541]$ orbital which provides $\Delta K = 1$ partners. This leads to large admixtures in the wave functions. The observed $\pi 3/2^-[532]$ state is at a lower energy than expected from the calculations. It is worth recalling that the model used has no adjustable parameters and that the excited states can have different deformations due to the influence of the particles coupled to the core on the nuclear deformation. However, in spite of the no particle-conservation limitation, the model has been a very good guide to interpret the experimental levels.

References

1. J. Sauvage *et al.*, Nucl. Phys. A **592**, 221 (1995).
2. A. J. Kreiner *et al.*, Phys. Rev. C **42**, 878 (1990).
3. D. Verney *et al.*, Eur. Phys. J. A **30**, 489 (2006).
4. J. Lettry *et al.*, in G.S. Bauer and R. Bercher, eds., ICANS-XIII, Joint Proc. 13th Meeting of the Int. Collaboration on Advanced Neutron Sources, PSI-Proc. 95-02, Villigen, Switzerland, p.595 (1995).
5. P. Kilcher *et al.*, Nucl. Instrum. Methods A **274**, 485 (1989), and references therein.
6. B. Roussière *et al.*, Nucl. Phys. A **643**, 331 (1998).
7. B. Roussière *et al.*, Hyperfine Interact. **129**, 119 (2000).
8. M. A. Cardona *et al.*, Eur. Phys. J. A **31**, 141 (2007).
9. B. Singh *et al.*, Nucl. Data Sheets **84**, 487 (1998).
10. G. Audi *et al.*, Nucl. Phys. A **729**, 3 (2003).
11. H. Somacal, Tesis de Doctorado, Universidad Nacional de Buenos Aires, Argentina (1996) and private communication.
12. F. Le Blanc *et al.*, Phys. Rev. C **60**, 054310 (1999).
13. S. Raman *et al.*, Nuclear Data Table **78**, 1 (2001).
14. C.J. Gallagher *et al.*, Phys.Rev. **111**, 1282 (1958).
15. L. Bennour *et al.*, Nucl. Phys. A **465**, 35 (1987).
16. D. Vautherin and D.M. Brink, Phys. Rev. C **5**, 626 (1972).
17. D. Vautherin, Phys. Rev. C **7**, 296 (1973).
18. H. Flocard *et al.*, Nucl. Phys. A **203**, 433 (1973).
19. M. Beiner *et al.*, Nucl. Phys. A **238**, 29 (1975).
20. M. Meyer *et al.*, Nucl. Phys. A **316**, 93 (1979).
21. K. Jentoft-Nilsen *et al.*, Phys. Rev. C **59**, 2422 (1999).
22. A. Zerrouki, Thèse, Université Paris-Sud, Orsay, (1979).
23. C. Schück *et al.*, Future directions in studies of nuclei far from stability, eds. J.H. Hamilton et al. (North-Holland, Amsterdam, 1980) p. 127.
24. C. Schück *et al.*, Rapport d'activité CSNSM (1978-1980) p.21.
25. U. Garg *et al.*, Phys. Lett. B **151**, 335 (1985).
26. S. André *et al.*, Phys. Rev. Lett. **38**, 327 (1977).
27. V.P. Janzen *et al.*, Phys. Rev. Lett. **61**, 2073 (1988).
28. G.D. Dracoulis *et al.*, Nucl. Phys. A **554**, 439 (1993).
29. R. Kaczarowski *et al.*, Phys. Rev. C **45**, 103 (1992).
30. H. Kawakami *et al.*, J. Phys. Soc. Jap. **36**, 623 (1974).
31. I.M. Ladenbauer-Bellis *et al.*, Can. J. Phys. **56**, 321 (1978).
32. A. Neskakis *et al.*, Nucl. Phys. A **261**, 189 (1976).
33. C. Fahlander *et al.*, Nucl. Phys. A **375**, 263 (1982).
34. B. Roussière *et al.*, Z. Phys. A **351**, 127 (1995).
35. B. Roussière *et al.*, Nucl. Phys. A **504**, 511 (1989).
36. J. Nyberg *et al.*, Nucl. Phys. A **511**, 92 (1990).
37. R.B. Firestone, Table of isotopes (John Wiley & Sons, New York, 1996).
38. M. H. Cardoso *et al.*, Z. Phys. A **272**, 13 (1975).
39. C. Schück *et al.*, Nucl. Phys. A **325**, 421 (1979).
40. R. A. Bark *et al.*, Phys. Lett. B **406**, 193 (1997).
41. F. Ibrahim *et al.*, Z. Phys. A **350**, 9 (1994).
42. B. Roussière *et al.*, Int. Conf. on Nuclear Structure and Related Topics, Dubna, Russia, June 2000. Nucl. Phys. of Russian Academy of Science **64**, 1210 (2001).
43. J. Sauvage *et al.*, Eur. Phys. J. A **25**, 5 (2005).
44. M.G. Porquet *et al.*, Nucl. Phys. A **411**, 65 (1983).
45. A. Ben Braham *et al.*, Nucl. Phys. A **482**, 553 (1988).
46. R. Bengtsson *et al.*, Nucl. Phys. A **327**, 139 (1979).
47. G. Levinton *et al.*, Phys. Rev. C **60**, 044309 (1999).
48. Ts. Venkova *et al.*, Eur. Phys. J. A **18**, 1 (2003).
49. D. Hojman *et al.*, Phys. Rev. C **61**, 064322 (2000).
50. R. A. Bark *et al.*, Nucl. Phys. A **630**, 603 (1998).
51. M. A. Cardona *et al.*, Phys. Rev. C **59**, 1298 (1999).
52. A. J. Kreiner *et al.*, Phys. Rev. C **40**, R487 (1989).